

JCU ePrints

This file is part of the following reference:

Carew, Michael John (2004) *Controls on Cu-Au mineralisation and Fe oxide metasomatism in the Eastern Fold Belt, N.W. Queensland, Australia*. PhD thesis, James Cook University.

Access to this file is available from:

<http://eprints.jcu.edu.au/17436>



CHAPTER 2:

***HYDROTHERMAL ALTERATION AND MINERALISATION
OF THE MOUNT FORT CONSTANTINE AREA:
IMPLICATIONS FOR THE EVOLUTION OF THE ERNEST
HENRY (CU-AU) SYSTEM***

HYDROTHERMAL ALTERATION AND MINERALISATION OF THE MOUNT FORT CONSTANTINE AREA: IMPLICATIONS FOR THE EVOLUTION OF THE ERNEST HENRY Fe OXIDE (Cu-Au) SYSTEM

2.1. INTRODUCTION

The Mount Fort Constantine exploration lease (MFC) has undergone significant exploration for Fe oxide (Cu-Au) mineralisation (IOCG) for more than twenty years. This heightened level of exploration has in the last decade been due to the lease's proximity to the Ernest Henry IOCG deposit, which represents the largest deposit of its kind in the Eastern Fold Belt (EFB) (Fig. 2.1). IOCG deposits in the district range from low to medium grade deposits (e.g. Ernest Henry, Mount Dore, Osborne) to small high-grade deposits (e.g. Mount Elliott/Starra and Eloise) and are highly variable in their mineralogical and geochemical character. Geochemical and mineralogical variability has been attributed to a diverse range of factors including pressure (P) and temperature (T), fluid composition (XCO₂, salinity), host rock composition, age and tectonic setting (Williams and Pollard, 2001). Au:Cu ratios are highly variable between deposits and are largely interpreted to reflect variations in fluid f_{O_2} (cf. Rotherham, 1997)

The relationships between hydrothermal alteration and Cu-Au mineralisation at MFC, Ernest Henry and other deposits in the Cloncurry district of the EFB are incompletely understood (Adshead, 1995; Baker, 1998; Rotherham, 1997; Mark et al., 1999). Does hydrothermal alteration and mineralisation at MFC represent a vector toward Cu-Au mineralisation at Ernest Henry, or are they reminiscent of 'background' alteration akin to the extensive regional alteration observed throughout the Cloncurry district? The primary focus of this chapter is to describe the geology and hydrothermal history in the MFC exploration lease by detailed logging of drill holes from two prospects (FC4NW and FC12) and mapping from nearby outcrop. This data will then be compared to previous work on the Ernest Henry (Cu-Au) deposit (Mark et al., 1999; Coward, 2001) to determine the relationship(s) between hydrothermal alteration at MFC and Fe oxide (Cu-Au) mineralisation at Ernest Henry.

2.2. GEOLOGY OF THE MOUNT ISA INLIER

The northern Australian Mount Isa Inlier is a complex Proterozoic terrane that has experienced a protracted tectonothermal history. Key aspects of this history, as

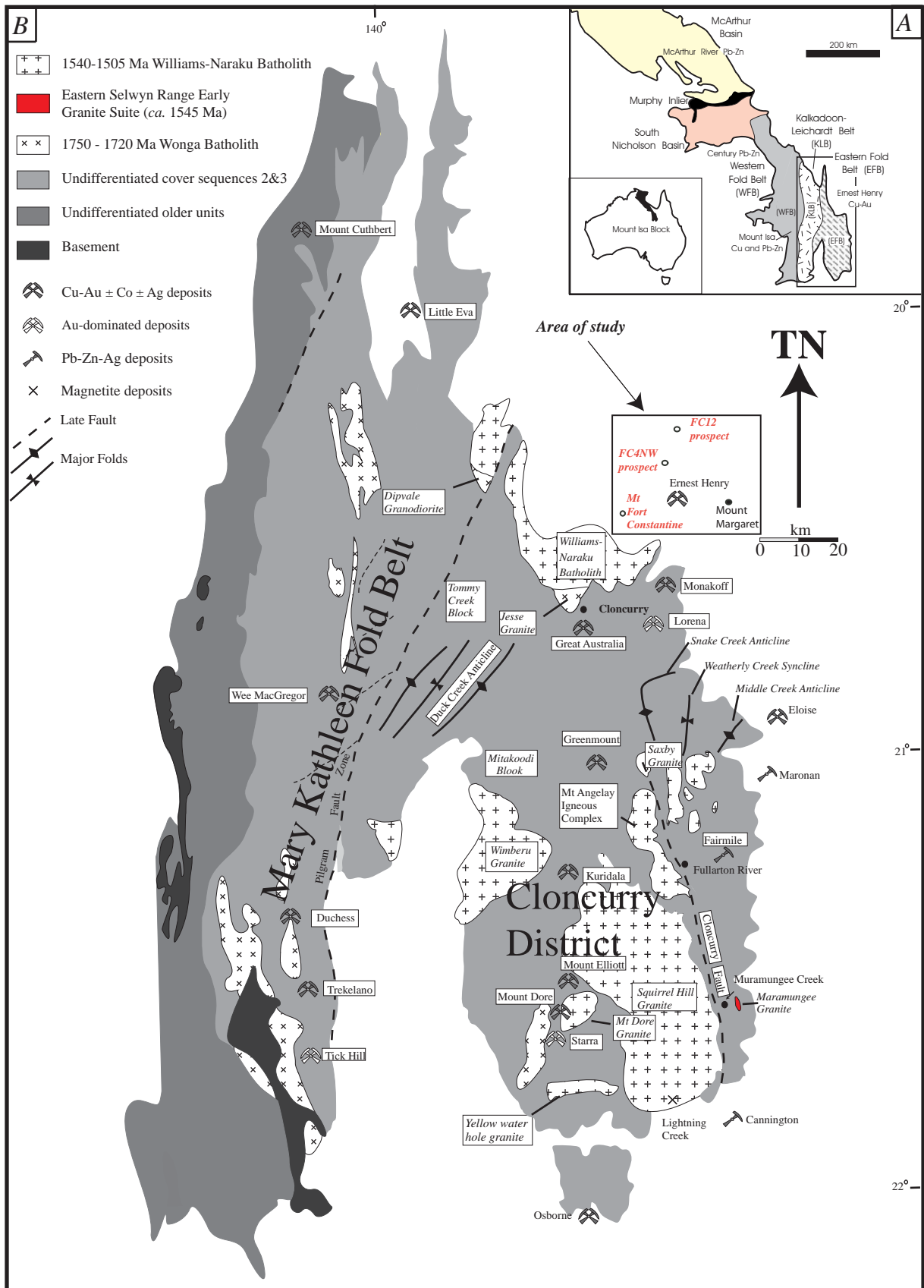


Figure 2.1. A. Tectonostratigraphic divisions of the Mount Isa Inlier, Queensland. B. Enlargement and simplified geology of the Eastern Fold Belt with localities of mineral deposits. Compiled from published AGSO maps and modified by Williams (1998). Includes locations of areas relevant to this study.

documented by previous workers, are summarized in the following section, with particular emphasis on the different styles of alteration and Cu-Au mineralisation in the EFB.

2.2.1 Regional tectonostratigraphic and igneous setting

The Palaeoproterozoic Mount Isa Inlier can be subdivided into the Eastern and Western Fold Belts (Page et al., 2000), which are separated by older Proterozoic basement (Blake, 1987). The Barramundi Orogeny (1890-1870 Ma; Blake, 1987) represents the earliest recorded deformation in the inlier and is mostly confined to basement rocks of Cover Sequence 1 in the central core of the Inlier (Blake, 1987). No exposed outcrop of basement rocks has been documented in the EFB. The Mary Kathleen Group (Cover Sequence 2; 1780-1725 Ma) is a mixed clastic-carbonate-evaporite metasedimentary sequence with some metavolcanic rocks (Derrick et al., 1976) overlying the 1783 Ma Argylla formation, predominately consisting of metavolcanic rocks. These are overlain by younger (~1672-1610 Ma) rocks of Cover Sequence 3, which are composed of clastic meta-sedimentary and volcanic metabasic rocks (Page and Sun, 1998).

The Wonga Batholith (1750-1720 Ma) represents the oldest intrusive event recorded in the EFB (Fig. 2.1). Intrusive phases of the batholith intrude Cover Sequence 2 rocks in the Mary Kathleen Fold Belt, and locally, in the Cloncurry district. It is composed of broadly contemporaneous granitoids and lesser mafic intrusions, as well as a 1754±25 Ma microgranite near Cloncurry (Dipvale Granodiorite) (Page and Sun, 1998). Isolated porphyritic intrusive bodies emplaced around 1740-1725 Ma also occur near the edge of the belt and these may be connected with a more extensive, but concealed metavolcanic sequence including those that host the Ernest Henry Cu-Au deposit (Page and Sun, 1998).

The Isan Orogeny (1600-1500 Ma) was the main orogenic event to affect post-Barramundi Orogeny rocks (Loosveld, 1989). The Maronan supergroup was thrust over the Mary Kathleen Group early during this time (D₁). Early authors suggested peak regional metamorphism to have occurred between 1550 and 1530 Ma (Page and Bell, 1986; Oliver et al., 1991; Rubenach and Barker, 1998), although later work suggests it occurred pre- to syn-D₂ in most parts of the Mount Isa Inlier at *ca.* 1590 Ma (Page and Sun, 1998; Rubenach et al., 2001, Giles and Nutman, 2002; Hand and Rubatto, 2002)

(Fig. 2.2). Across the inlier, the peak regional metamorphic grade varies from greenschist to upper amphibolite facies (Jacques et al., 1982; Foster and Rubenach, 2001).

The Williams and Naraku Batholiths are associated with several later deformation phases involving ductile shear zones, brittle-ductile shear zones and brecciation (D_3), and contain intrusions belonging to at least three different age groups (Perkins and Wyborn, 1998; Pollard et al., 1998). This includes a small, K-rich microgranite of *ca.* 1550 Ma, a suite of foliated and altered granites including Na-rich trondhjemite bodies at *ca.* 1540 Ma, and younger intrusions composed of diorite, monzonite, tonalite, granodiorite, granite and alkali granite (Perkins and Wyborn, 1998; Pollard et al., 1998). These younger intrusions have crystallisation ages ranging between 1540-1505 Ma (Page and Sun, 1998) (Fig. 2.2).

2.2.2. Metasomatism and mineralisation in the Mount Isa Inlier

Regional-scale metasomatism is well documented throughout the Mount Isa Inlier (de Jong and Williams, 1995; Oliver, 1995; Mark and De Jong, 1996; Mark, 1998a, b), and is manifested as a series of spatially overlapping suites of alteration that occurred over a protracted period (Mark, 1998a,b; Oliver et al., 2001). Three major categories of alteration relevant to this study can be described and include early $\text{Na}\pm\text{Ca}$ alteration and skarns associated with the Wonga Batholith (D_e), syn- to post-regional metasomatic alteration associated with the Isan orogeny (D_1 to D_2), and syn- to post- regional metamorphic alteration associated with the Williams and Naraku Batholith (D_3).

Early Wongan metasomatism (ca. 1740 Ma)

Oliver et al (1994) recognised an early alteration event (D_e) in the Mary Kathleen Fold Belt (Fig. 2.3). This early phase contains many features reminiscent of similar alteration suites observed by Vanko and Bishop (1982) and Barton and Johnson (2000) in the Humbolt Lopolith in Nevada. Metasomatism is interpreted to involve the circulation of hot hyper-saline fluids and the production of Na-scapolite synchronous or slightly predating the development of garnet-pyroxene-scapolite skarns proximal to granitoids (Oliver et al., 1994). In the Mary Kathleen Fold Belt, this fluid circulation is attributed

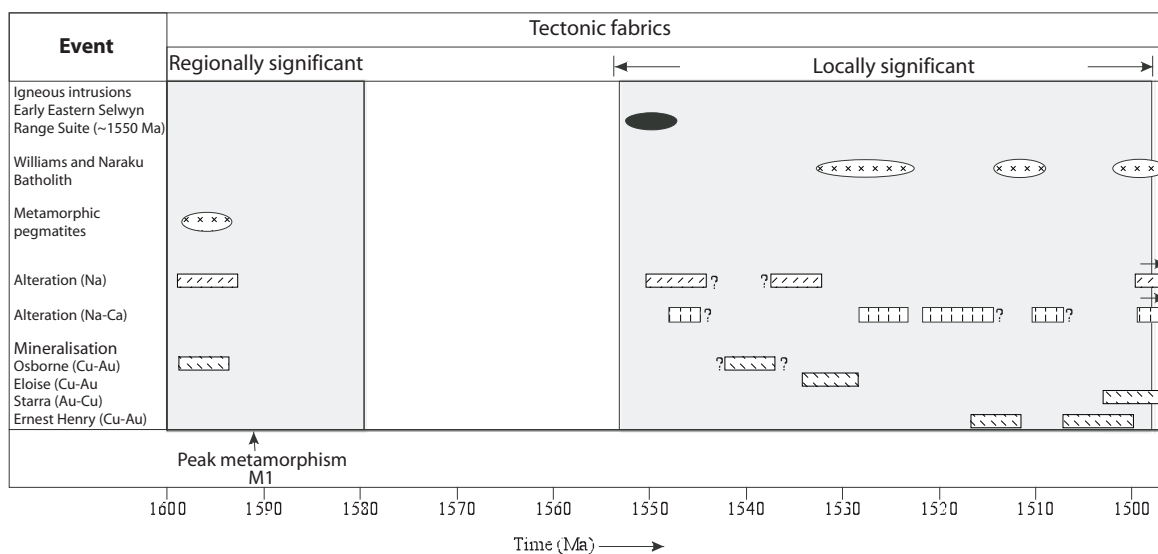


Figure 2.2. The temporal distribution of post-Wonga magmatism, tectonism, metamorphism, alteration and Cu-Au mineralisation in the Cloncurry District (modified after Mark et al., 1999).

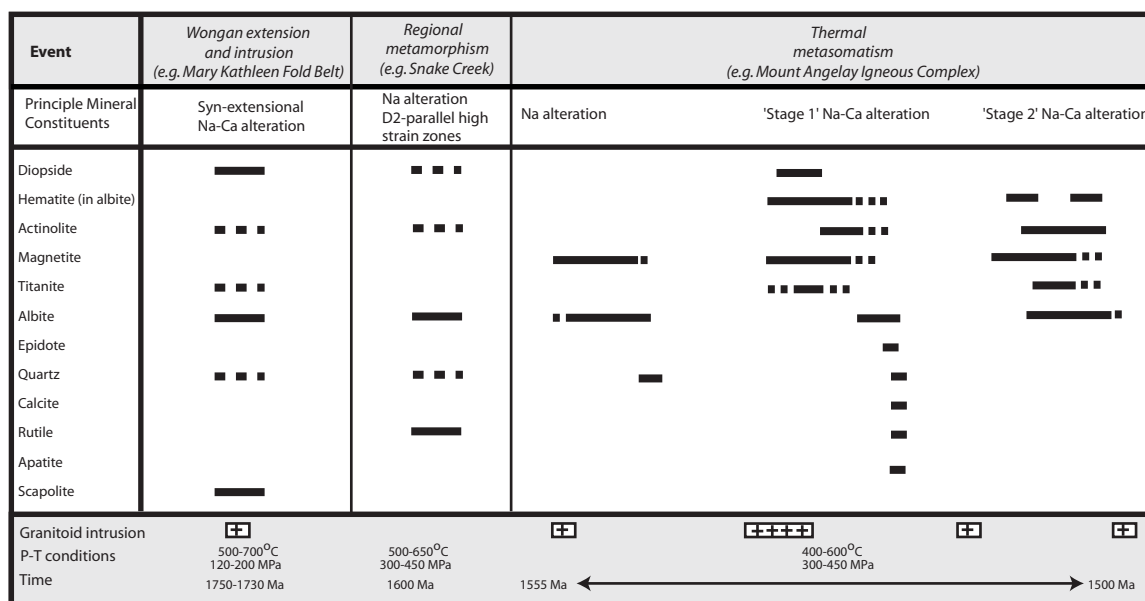


Figure 2.3. Paragenetic chart showing the major mineral assemblages observed from regional Na-Ca alteration with respect to major deformation, metamorphism and igneous events in the Eastern Fold Belt, incorporating data from the following sources: Oliver et al (1994); Adshead (1995); Oliver (1995); Mark (1998a); Pollard et al (1998); Rubenach and Barker (1998); Oliver et al (1999); Foster and Rubenach (2001); Rubenach et al (2001); Giles and Nutman (2002); Rubenach and Lewthwaite (2002).

to the emplacement of the Wonga Batholith magmas at *ca.* 1740 Ma (Oliver et al., 1994; Oliver, 1995; Oliver et al., 1999) and is supported by $\delta^{18}\text{O}$ values that range between 7 to 12 ‰. The petrology and mineralogy of the alteration suites suggest that they developed at temperatures of 500-700 °C and pressures of 150-200 MPa (Fig. 2.3). This early Na alteration predates the deposition of metapelitic rocks of the Soldiers Cap Group.

Regional metamorphic metasomatism (ca. 1600-1500 Ma)

Albitisation of metapelitic rocks from the Soldiers Cap Group at the Osborne Cu-Au deposit and Snake Creek area occurred during the Isan orogeny (D₁ and D₂) between 1600-1580 Ma (Adshead, 1995; Rubenach and Barker, 1998; Rubenach et al., 2001; Rubenach and Lewthwaite, 2002). Albitisation of these rocks occurred during the initial stages of regional metamorphism at approximately 500 to 650 °C and 300 to 450 MPa (Fig. 2.3) (Rubenach and Lewthwaite, 2002), and is predominantly structurally controlled within shear zones that cut bedding. Although alteration exhibits no apparent temporal association with any major intrusions, abundant abyssal pegmatites with surrounding albitisation are observed at Osborne and may be genetically linked.

Syn-intrusive (Williams and Naraku) metasomatism (1550-1480 Ma)

Na±Ca alteration

Albite alteration occurs in retrograde (D₃) brittle-ductile shear zones and brittle Na-Ca-bearing fracture and mega-breccia systems that formed along regional fault systems synchronous with the emplacement of the Williams and Naraku Batholith (1550-1500 Ma; Fig. 2.2, 2.3) (Oliver et al., 1990; Williams, 1994; de Jong and Williams, 1995; Oliver, 1995; Mark, 1998a, b, Marshall, 2003). In the Mary Kathleen Fold Belt, intense zones of veining and brecciation and related albite alteration affect approximately 20% of all exposed rocks. In comparison, albite alteration in the Cloncurry district is very widespread in both the Corella Formation and Mary Kathleen Group equivalents, but is also common in Soldiers Cap Group pelitic rocks. Common Na-Ca-bearing mineral assemblages include albitic plagioclase + actinolite + titanite ± quartz ± calcite ± magnetite ± clinopyroxene (diopside).

Na-Ca mineral assemblages can vary greatly, as demonstrated by de Jong and Williams (1995) at the Muramungee Creek and Fullarton River gorge, in the vicinity of the Cloncurry Fault north east of the Selwyn Range. De Jong and Williams (1995) noted that Na-Ca assemblages at Fullarton River gorge contain a dominant clinopyroxene-rich assemblage, compared to amphibole-rich assemblages at Muramungee Creek. De Jong and Williams (1995) suggested that clinopyroxene-rich Na-Ca alteration assemblages from Fullarton River formed under more reduced pressures highlighted by brittle-style veining, in addition to elevated temperatures and/or diminished XCO₂.

Perhaps the most striking example of the relationship between intrusive complexes and regional Na-Ca alteration is present at the Mount Angelay igneous complex (Fig. 2.1). Here the association of hydrothermal veins formed from Na-Ca fluids, and UST (unidirectional solidification textures) similar to those observed in evolved, apical portions of porphyry Cu-Mo deposits, suggests a direct genetic role for granites during hydrothermal alteration (Mark, 1999). Three broad phases of Na-Ca alteration have been documented and include early Na alteration, stage 1 Na-Ca alteration and stage 2 Na-Ca alteration. (Mark, 1998a) (Fig. 2.3).

Around the Mount Angelay igneous complex, estimated temperatures from oxygen isotope geothermometry (magnetite, quartz and albite) suggest Na-Ca alteration evolved from parent magmas at >510°C, to differentiated low temperature pegmatites in equilibrium with albite at 550-500°C, through to igneous derived hydrothermal breccias and associated Na-Ca alteration at around 500 to 400°C (Tolman, 1998; Mark and Foster, 2000). Early Na alteration typically contains albite, magnetite and minor quartz (Fig. 2.3) (Mark, 1998a; Mark, 1999). Stage 1-style Na-Ca alteration consists of albite, actinolite, diopside, epidote, magnetite, titanite and minor late calcite, rutile and quartz. Mineral proportions change over time, with diopside occurring early as the dominant calc-silicate mineral, progressing to actinolite-epidote-calcite-rutile and quartz-rich assemblages (Fig. 2.3) (Mark, 1998a; Mark, 1999). Veins and dykes associated with this phase contain both magmatic and hydrothermal components, where pegmatite and aplite form the substrate for hydrothermal minerals (e.g. actinolite, albite and apatite). Stage 2-style Na-Ca alteration (actinolite, albite, magnetite, titanite, and apatite) is more distal within surrounding country rocks and cuts intrusive rocks

genetically related to stage 1-style Na-Ca alteration. Na-Ca alteration associated with stage 2 at Mount Angelay is reminiscent of typical Na-Ca alteration scattered throughout the EFB (Mark, 1998a; Mark, 1999) (Fig. 2.3).

Fe oxide (\pm Cu-Au) mineralisation

On a broad scale (10 to 100's m), an association between post-D₂ phases of the Williams and Naraku Batholith and Fe oxide (Cu-Au) mineralisation is evident (Fig. 2.2). However, it is difficult to link individual plutons or alteration types to economic ore deposits (Wyborn, 1992). In general, the spatial relationship between IOCG deposits and granitoids is distal, in contrast to the more thoroughly understood porphyry Cu-Au-type deposits. In terms of potential pathways for granite-derived hydrothermal fluids, fracture-induced permeability through both breccia and fault zones is likely to have been the main means of fluid migration (Wyborn and Heinrich, 1993; Marshall, 2003). Numerous barren Fe oxide-rich rocks also occur throughout the EFB, some of which appear spatially and temporally associated with IOCG deposits (e.g. Fe-K alteration at Starra Au-Cu, Osborne Cu-Au and Ernest Henry Cu-Au). The majority of Fe oxide-rich rocks in the Cloncurry district, however, bear no spatial relationship to Fe oxide Cu-Au mineralisation. A more thorough description of the major IOCG occurrences in the EFB is discussed in detail in Chapter 5.

2.3. THE ERNEST HENRY Fe OXIDE CU-AU DEPOSIT

The Ernest Henry ore body is predominately hosted in felsic metavolcanic rocks originally composed of fine- to medium-grained plagioclase phenocrysts in a fine-grained plagioclase-rich groundmass (Mark et al., 1999). Other rock types found within and adjacent to the Ernest Henry deposit include:

- Metasedimentary rocks, which are typically fine-grained muscovite-biotite psammite composed of biotite, quartz, muscovite and plagioclase, occur predominately to the west of the deposit. Rare scapolite-bearing calc-silicate rocks are also observed (Mark et al., 1999).
- Metadiorite intrusions metamorphosed to amphibolite facies and composed of hornblende, plagioclase, magnetite, quartz and rare K-feldspar (Mark et al., 1999). Two major dioritic intrusions occur to the northwest and south of the deposit and

have U-Pb and titanite crystallisation ages of 1660-1650 Ma (Pollard and McNaughton, 1997)

The host sequence at Ernest Henry is foliated, with the intensity of fabric development increasing towards the hanging wall of the SE dipping, S- to SSE- plunging orebody (Ryan, 1998). The footwall represents a change downward from brecciated felsic volcanic rocks, to sheared, strongly foliated rocks that are variably brecciated. The foliation(s) (oriented parallel to the sheared contacts of the hanging wall and footwall) anastomose around boudinaged breccia clasts formed during earlier Cu-Au mineralisation (Mark et al., 1999).

Hydrothermal alteration within and surrounding the Ernest Henry deposit can be divided into six mineral associations applicable to this study:

1. Regional Na-Ca alteration: Occurs as albitic plagioclase-magnetite-clinopyroxene-amphibole-rich veining, fault-related breccia fill and associated alteration. This style of alteration has been documented throughout the EFB (de Jong and Williams, 1995; Oliver, 1995; Mark, 1998a,b) (Section 2.2).
2. Pre-ore early Kiruna-style Fe oxide-rich rock: Located within the hanging wall of the deposit and exhibit a similar mineralogy to Na-Ca alteration suggesting a genetic link (Mark *pers comm*).
3. Fine-grained biotite-magnetite alteration: Is particularly intense in volcanic rocks peripheral to the Ernest Henry ore body. The origin of this alteration is difficult to discriminate although minor cracks filled with biotite and magnetite suggests a hydrothermal alteration.
4. 'Red-rock' hematized K-feldspar alteration: Fine-grained replacement of both plagioclase within the host rocks and of earlier albite alteration. Occurs as multiple alteration phases that may pre- and post-date Cu-Au mineralisation (6). This alteration is associated with quartz, calcite, magnetite, fluorite and titanite vein infill.
5. Garnet-K-feldspar-biotite veining and alteration: The rocks affected by this alteration typically occur within the footwall of the deposit. This alteration phase also exhibits a close spatial and chemical relationship to Cu-Au mineralisation suggesting a genetic relationship (Mark et al., 1999).

6. Cu-Au mineralisation: Associated with two distinct events. The first, and major, ore-forming event is associated with brecciation, with the matrix largely composed of magnetite, calcite, pyrite, biotite, chalcopyrite, K-feldspar, titanite and quartz. The second event is similar in mineralogy, but is contained in a network of veins that cut the earlier mineralised breccias (Mark et al., 1999). Late carbonate flooding postdates Cu-Au mineralisation, and is restricted to rocks in the footwall of the deposit (Mark et al., 1999).

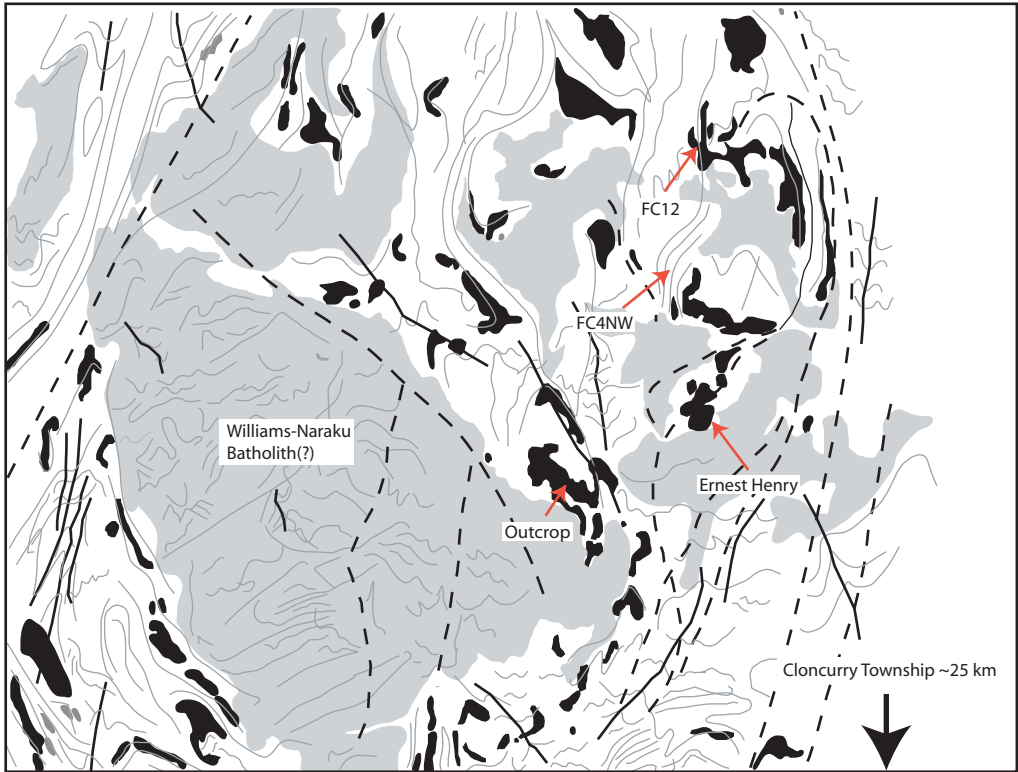
The hydrothermal activity associated with Cu-Au mineralisation largely post-dates regionally extensive Na-Ca alteration, suggesting there were probably two hydrothermal systems that overlapped in space (Mark et al., 1999). The K-feldspar-, magnetite-, calcite- and garnet-rich mineralogy and K-, Ba-, Mn-rich chemistry of Ernest Henry exhibits some chemical characteristics similar to other IOCG deposits (e.g. Monakoff; Davidson and Davis, 1997). However, Cu-Au mineralisation is not related to the replacement of previous Fe oxide-rich rocks as interpreted for the Starra Au-Cu deposit (Rotherham, 1997) and Osborne Cu-Au deposit (Adshead, 1995; Banvill, 1998). Most of the magnetite within the ore body at Ernest Henry was deposited during and/or slightly before sulphide mineralisation (Mark et al., 1999).

2.4. GEOLOGY OF THE MOUNT FORT CONSTANTINE DISTRICT

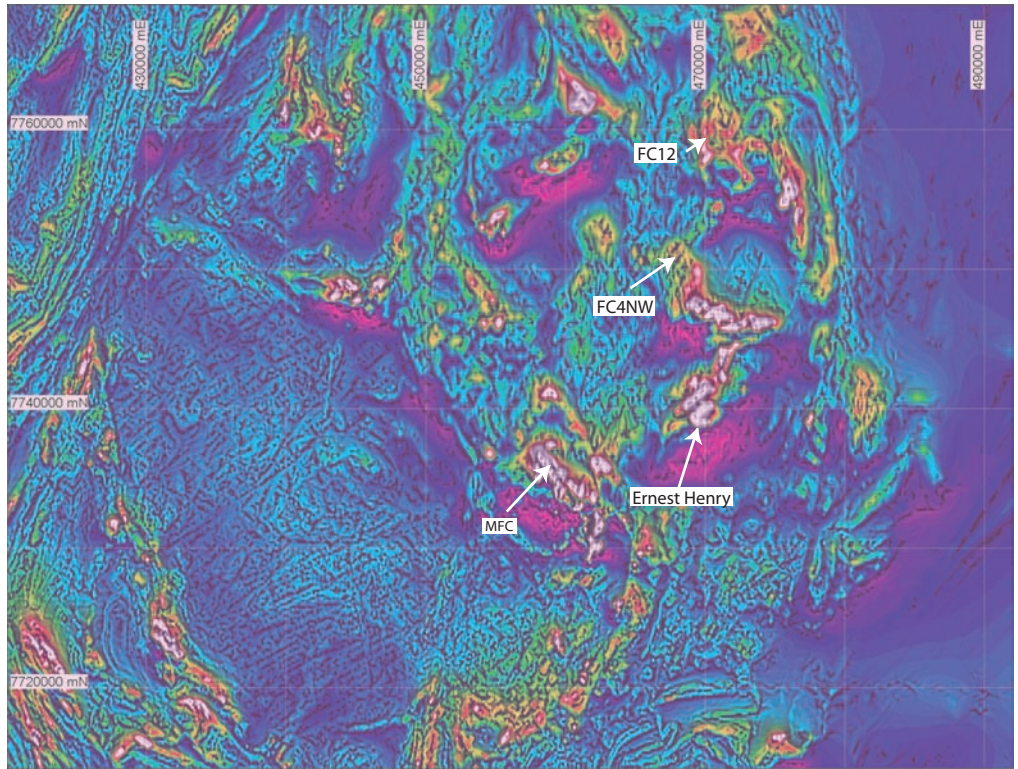
The MFC exploration lease comprises one main area of outcrop and two prospects defined by drilling (FC12 and FC4NW prospects), which were explored by MIM Exploration (now Xstrata) to investigate the potential for Fe oxide (Cu-Au) mineralisation (Fig. 2.4). All areas occur within 10-20 km of the Ernest Henry Cu-Au deposit, and are adjacent to or situated on highly magnetic areas defined by aeromagnetic data. Diamond drill holes from the FC12 and FC4NW prospects were logged, and results were constructed into two cross-sections, one north-south and one east-west trending (Fig. 2.5, 2.6). These cross-sections illustrate the spatial distribution of the regional alteration styles and provide means to constrain the temporal and spatial relationship between hydrothermal alteration and mineralisation. They also provide a

Figure 2.4. Aeromagnetic interpretation of the MFC exploration lease and surrounding area. Areas relevant to this study including MFC outcrop, the FC4NW and FC12 leases, and the Ernest Henry Cu-Au deposit are shown. Grey zones are areas of low magnetic response and are interpreted to be major intrusive units. Black zones are areas of high magnetic response and include the Ernest Henry Cu-Au deposit and the FC12 lease. Interpreted folds and faults are also shown. Note the bend (inferred dilatant jog) associated with the Ernest Henry deposit expressed as a magnetic high.

A



B



legend

- Igneous intrusions
- Fe oxide-rich rocks

- Interpreted axial planes of folds
- Deformation (folds/fabric)
- Major faults

10 km

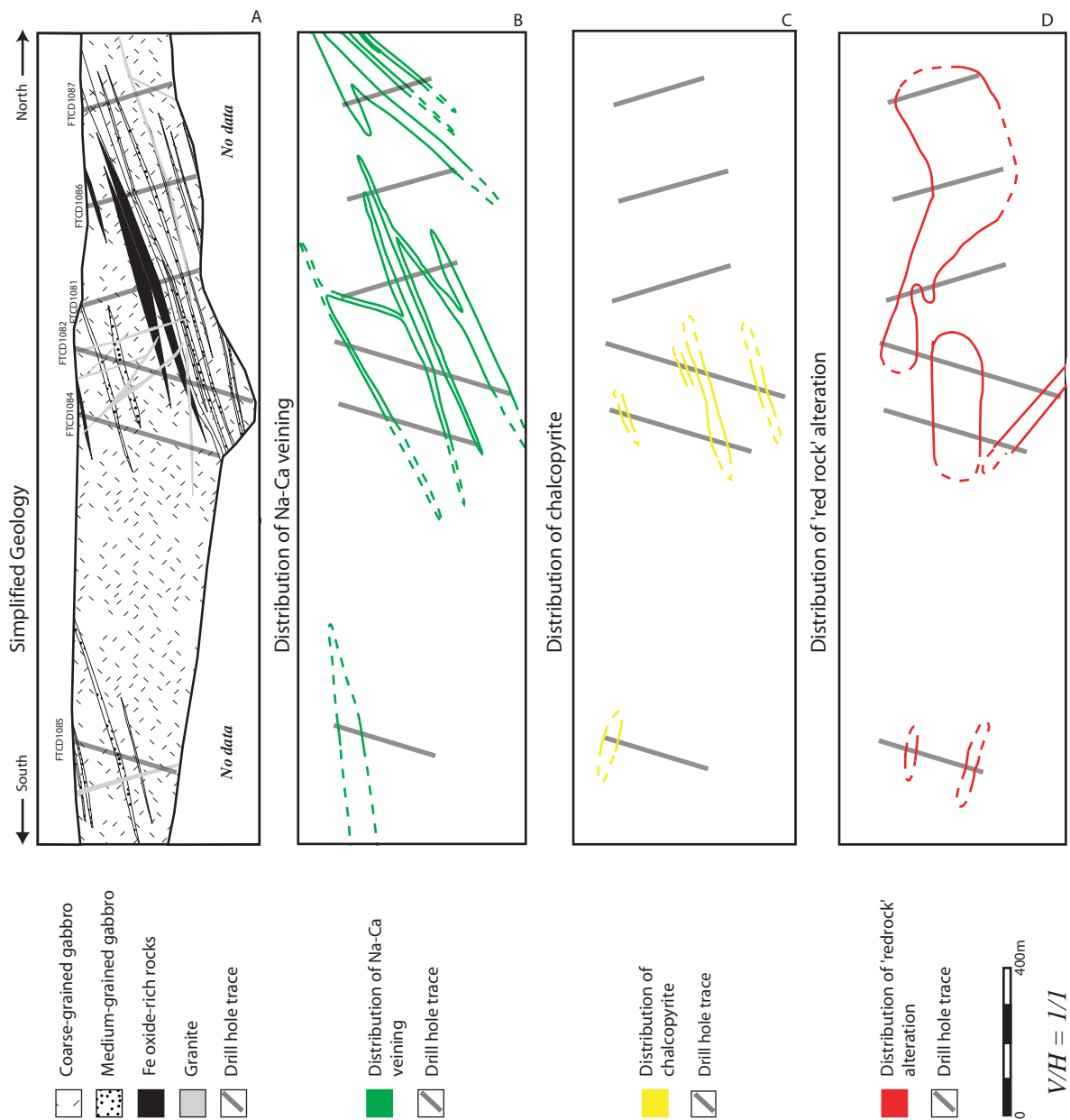


Figure 2.5. Interpreted geological cross-sections illustrating the distribution of rock types, alteration phases and minerals at the FC12 lease:

- A. rock types.
- B. Na-Ca veining.
- C. chalcopyrite.
- D. 'red rock' alteration.

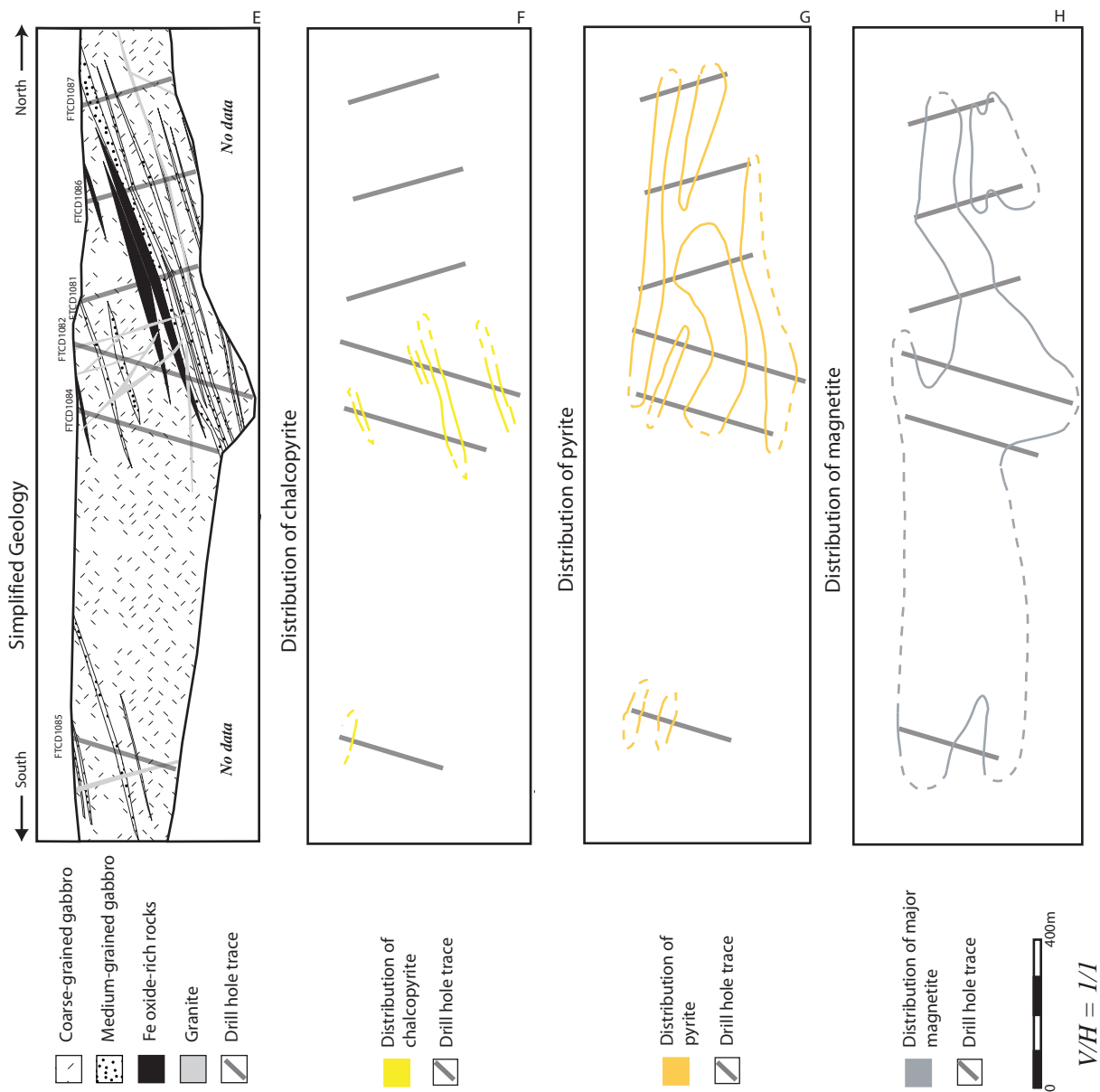


Figure 2.5. Interpreted geological cross-sections illustrating the distribution of rock types, alteration phases and minerals at the FC12 lease:

- E. rock types.
- F. chalcopyrite.
- G. pyrite.
- H. magnetite.

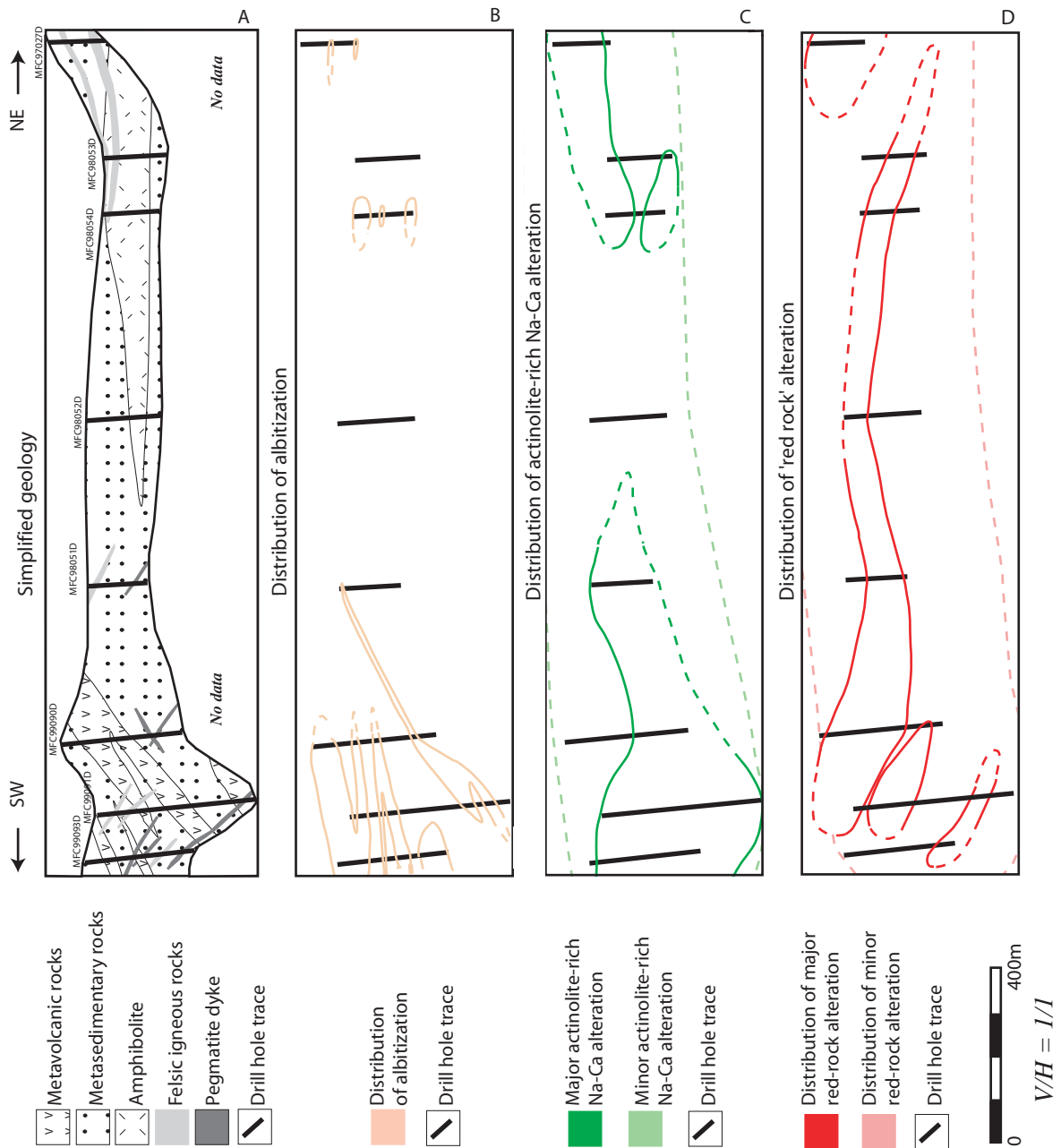


Figure 2.6. Interpreted geological cross-sections illustrating the distribution of rock types, alteration phases and minerals at the FC4NW lease:

A. rock types.

B. albittisation.

C. clinopyroxene-rich Na-Ca alteration.

D. 'red rock' alteration.

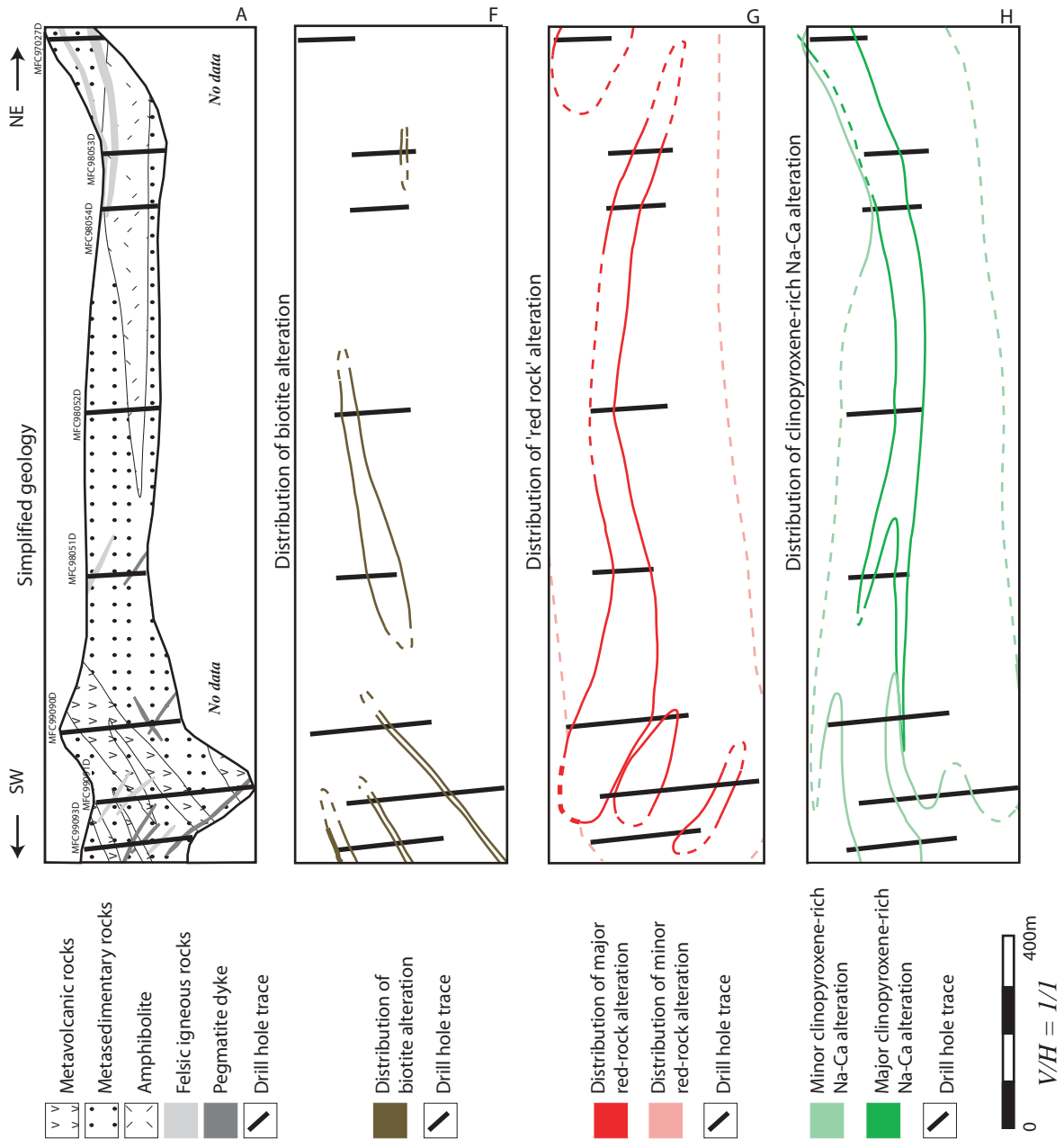


Figure 2.6. Interpreted geological cross-sections illustrating the distribution of rock types, alteration phases and minerals at the FC4NW lease:

E. rock types.

F. biotite-amphibole alteration.

G. 'red rock' alteration.

H. clinopyroxene-rich Na-Ca alteration.

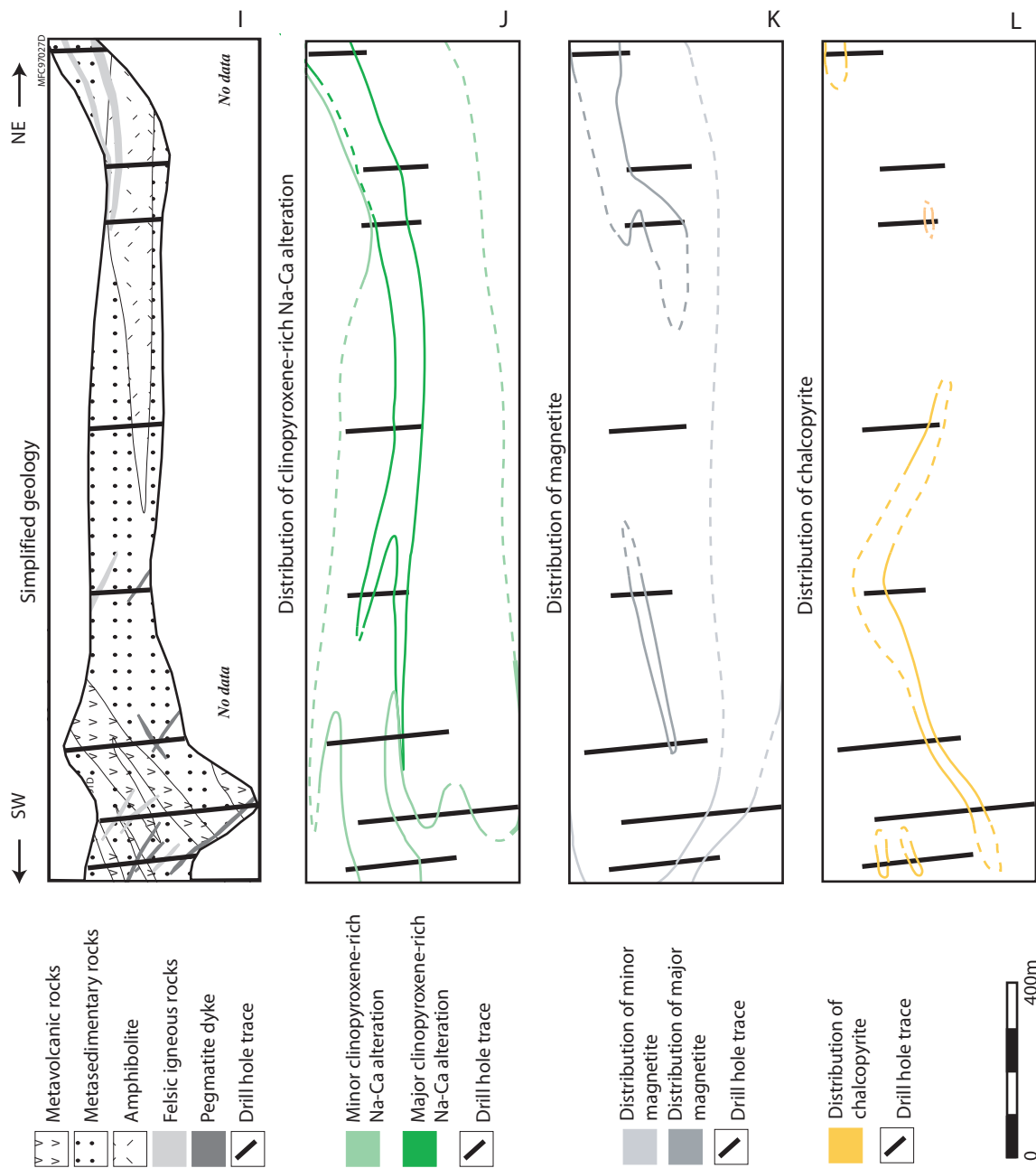


Figure 2.6. Interpreted geological cross-sections illustrating the distribution of rock types, alteration phases and minerals at the FC4NW lease:

I. rock types.

J. clinopyroxene-rich Na-Ca alteration.

K. magnetite.

L. chalcopyrite.

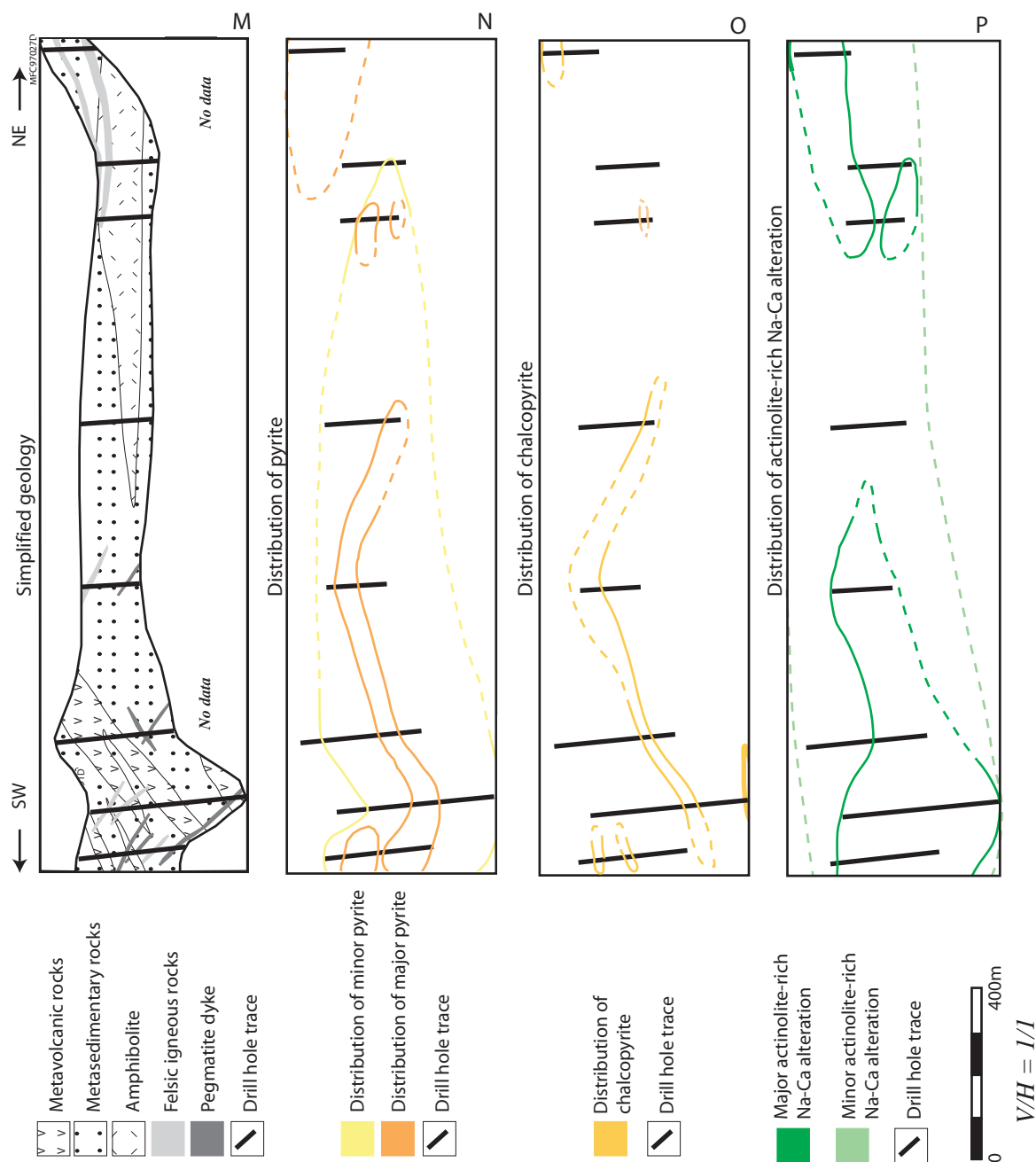


Figure 2.6. Interpreted geological cross-sections illustrating the distribution of rock types, alteration phases and minerals at the FC4NW lease:

M. rock types.

N. pyrite.

O. chalcopyrite.

P. amphibole-rich Na-Ca alteration.

useful framework for determining the important ingredients and conditions associated with sulphide mineralisation, and the specific relationships to the Ernest Henry Cu-Au deposit. The FC12 prospect is located *ca.* 20 km north of the Ernest Henry deposit (Fig. 2.4). The area exhibits a significant magnetic high where 6 diamond holes were drilled over a 2 km length. Two holes were drilled at an angle of 60° to the west, whilst the remaining holes were drilled at the same plunge towards the east. Using structural data including core axis angles of the boundaries of various alteration phases, north-south oriented cross-sections were constructed and are presented in figure 2.5. The FC4NW prospect is situated on an area of moderate magnetic intensity (Fig. 2.4), and is located *ca.* 10 km north of the Ernest Henry deposit. Eight holes were drilled over a length of 1.7 km, where each hole was oriented at 60-70° toward the southeast, with the exception of hole MFC99092D, which was drilled towards the northwest. Cross-sections were constructed from these drill holes (excluding hole MFC99092) using drill core angles and structural relationships from partly oriented core (Fig. 2.6). Finally, a geological map (*ca.* 2×2 km) was constructed from an area of outcrop located 10 km SW of Ernest Henry. This area is dominated by plagioclase-quartz phyric felsic volcanic rocks affected by Na-Ca and K alteration (Fig. 2.7).

2.5. ROCK TYPES

A number of rock types were documented in the MFC exploration lease. Quartz-plagioclase phyric felsic volcanic rocks, similar to those that host Cu-Au mineralisation at the Ernest Henry deposit, are abundant in outcrop. In contrast, feldspar-phyric felsic volcanic rocks are the dominant rock type within the FC4NW prospect, whereas medium- to coarse-grained tholeiitic gabbroic rocks are the dominant rock type in the FC12 prospect. Other rock types observed are fine-grained calc-silicate rocks (FC4NW, outcrop), fine- to medium- grained pelitic-psammitic metasedimentary rocks (FC4NW), amphibolite (FC4NW) and Fe oxide-rich rocks of various affinities (outcrop, FC4NW, FC12). Younger felsic intrusions are common at FC4NW and FC12, while a young diorite dyke post-dating alteration was observed in outcrop.

2.5.1. Metavolcanic rocks

The MFC felsic volcanic rocks have previously been interpreted to represent a sequence of intrusive and extrusive rocks related to waning extension at the end of

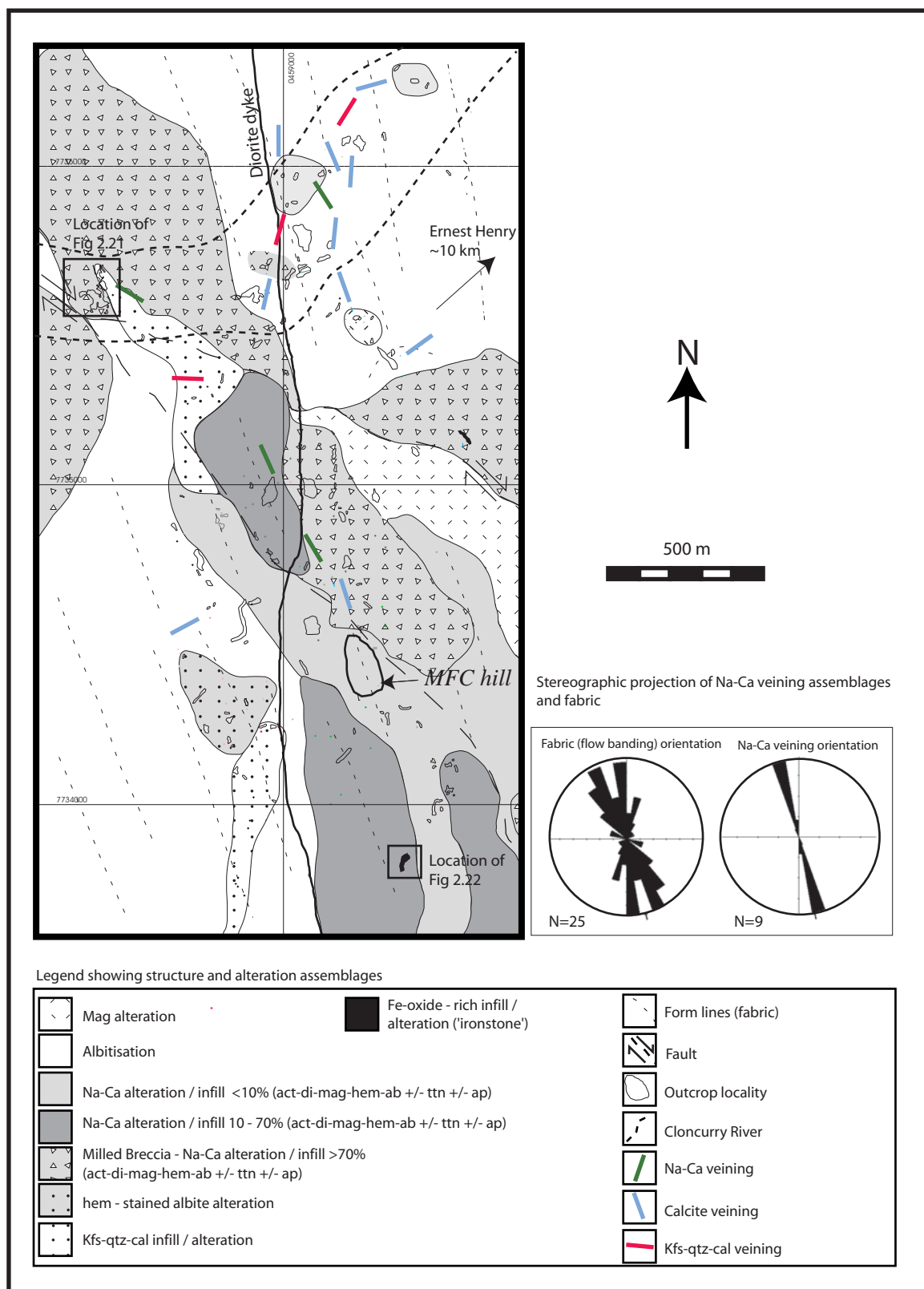


Figure 2.7. Interpreted geological map showing the distribution of alteration in outcrop at MFC. The total exposed outcrop = <5 %, and a combination of geological mapping and geophysical interpretation were used to construct interpreted boundaries. Note two SE-NW trending faults that may have acted as conduits for fluids associated with Na-Ca and K alteration. act=actinolite, di=diopside, mt=magnetite, hem=hematite, ab=albite, ttn=titanite, ap=apatite, cal=calcite, qtz=quartz, Kfs=K feldspar, mag=magnetite. Abbreviations after Kretz (1983).

deposition of Cover Sequence 2 (Craske, 1995). Page and Sun (1998) determined U-Pb zircon ages of 1746 ± 9 Ma, 1742 ± 6 Ma and ca.1740 Ma for three highly altered and brecciated metavolcanic rocks from outcrop at MFC. Previous work on the MFC volcanic rocks by Blake et al (1997) categorised these rocks into three main groups: trachytic-textured feldspar porphyry; microcline-rich andesite; and mylonitic, K-altered andesite. These categories are, however, based on the assumption that the observed K-feldspar is primary, and hence have not been employed in this study. The extent to which the metavolcanic rocks occur on a regional scale is unclear, however, they are bound to the west by a large magnetic low (Fig. 2.4), interpreted to be part of the Williams-Naraku Batholith. Minor granite outcrop is located to the west of the area of outcrop, supporting this interpretation. Work by Mark (*pers comm.*) indicates that felsic volcanic rocks occur north of the FC12 prospect, while Marshall (*pers comm.*) also documented felsic volcanic rocks to the south of the Ernest Henry deposit, east of Cloncurry.

Examples of unaltered metavolcanic rocks from FC4NW are rare (Fig. 2.8b), however except for the presence of quartz phenocrysts, their composition appears to be broadly similar to unaltered samples in outcrop (Fig. 2.8d). The metavolcanic rocks typically have a fine-grained dark grey to black matrix composed of plagioclase (45-50 %), quartz (30-40 %) and magnetite (1-2 %). Quartz and plagioclase phenocrysts are typically <1-3 mm, with the quartz phenocrysts commonly partially recrystallised. The proportion of phenocrysts is highly variable, although typically ranging between 5-10 modal %. Blake et al (1997) suggested that these rocks represent coherent lavas and/or high-level intrusive rocks.

Post-depositional processes including alteration, metamorphism, and deformation have affected most of the volcanic sequence in outcrop and in the FC4NW prospect (Fig. 2.8a,b, 2.9, 2.10 and 2.11). A N-S trending fabric and sub-vertical dip is common in outcrop, and suggests a broad tectonic fabric produced by post-emplacement processes potentially associated with regional east-west compression. While the consistent north-south orientation implies the fabric is tectonic, the alignment of quartz and plagioclase phenocrysts in thin section suggests that it may be a product of primary flow banding (Fig. 2.11a), which may have been modified by a later deformation event. Aeromagnetic data (Fig. 2.4) indicates this fabric is refracted around a magnetic low,

Figure 2.8. Photographs of rock types from the FC4NW prospect.

A. Folded intercalated plagioclase phyrlic felsic volcanic rock and metasedimentary rock cut by thin actinolite-magnetite-chalcopyrite-albite vein. This vein is affected by later hematite-stained K-feldspar alteration. MFC97027, 47.2m.

B. Plagioclase phyrlic felsic volcanic rock cut by actinolite + magnetite + pyrite + chalcopyrite + albite veins. Notice hematite-stained K-feldspar alteration replacing albite alteration associated with an amphibole-rich Na-Ca vein. MFC99091, 469.7m.

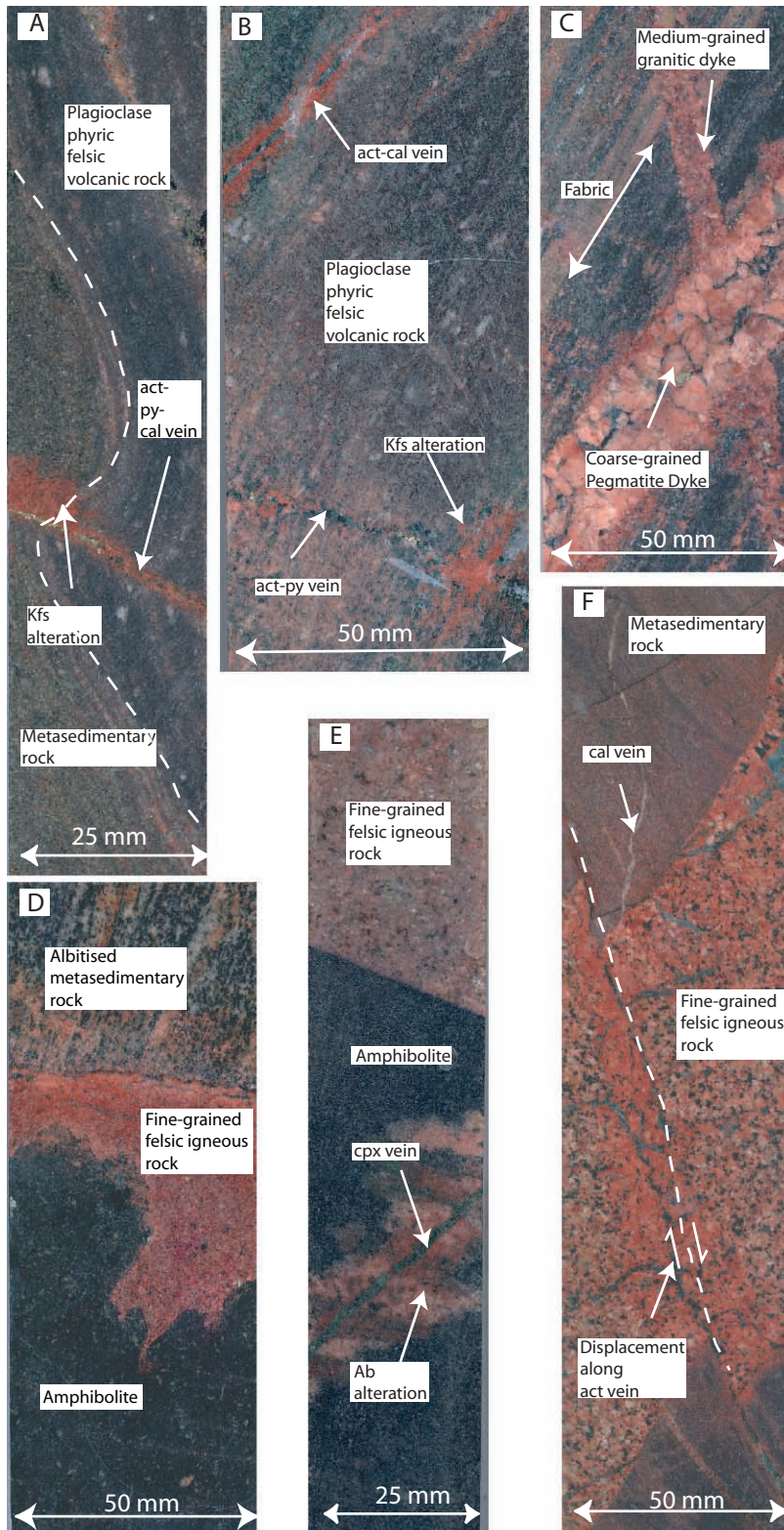
C. Metasedimentary rock cut by an albitised felsic igneous rock, which is later overprinted by a pegmatite dyke. Note that the albitisation of the metasedimentary rock utilises a pre-existing tectonic fabric. MFC99092, 285.4 m.

D. A contact between an amphibolite and an albitised felsic igneous rock. The irregular contact may indicate magma mingling between the two rock types. MFC99093, 127 m.

E. Fine-grained amphibolite cut by an albitised felsic igneous rock subsequently overprinted by a later diopside + albite + magnetite vein. MFC98052, 211.4 m.

F. Metasedimentary rock cut by an albitised felsic igneous rock. Note the albitisation along bedding and the displacement of the felsic igneous rock along an actinolite + magnetite + pyrite + chalcopyrite + albite Na-Ca vein. MFC97012, 81.2 m.

Abbreviations: Kfs=K feldspar, act=actinolite, ttn=titanite, ab=albite, hem=hematite, qtz=quartz, mag=magnetite, ccp=chalcopyrite, cal=calcite, py=pyrite. Abbreviations after Kretz (1983)



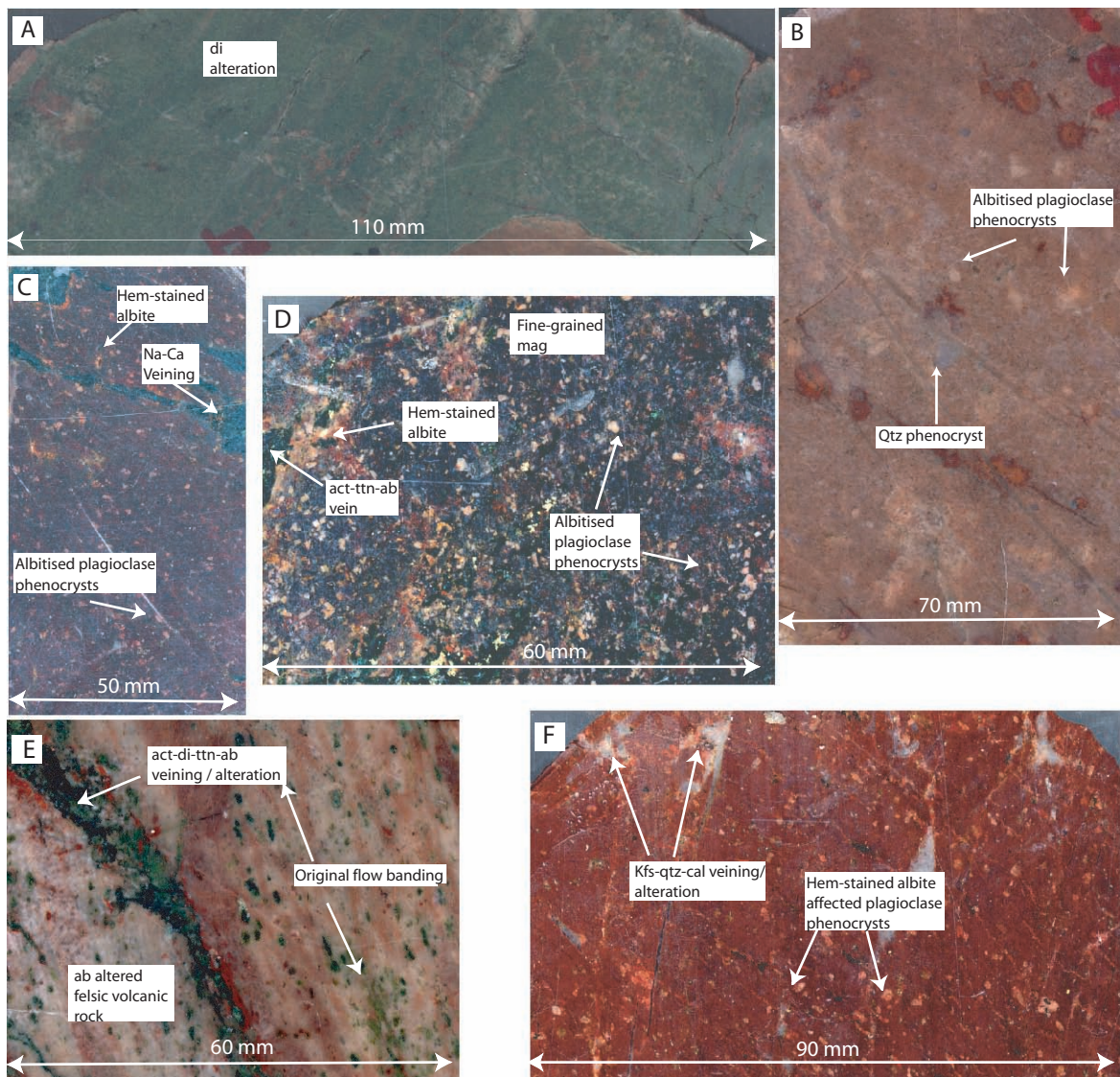


Figure 2.9. Photographs of rock types observed in outcrop at MFC.

A. Fine-grained calc-silicate rock altered by intense Na-Ca alteration. 80-85 % of the rock is composed of diopside. MFC17.

B. Quartz-and plagioclase-phyric felsic volcanic rock affected by albitisation. MFC outcrop, MFC15.

C. Plagioclase-phyric felsic volcanic rock with fine-grained matrix affected by albitisation and later hematite-stained albite alteration. MFC013003.

D. Plagioclase phyric felsic volcanic rock with albitised plagioclase phenocrysts and minor hematite-stained albite alteration. MFC70.

E. Plagioclase-phyric felsic volcanic rock affected by intense Na-Ca alteration. Note vertical trend in rock defined by relict phenocrysts that may represent original flow banding. MFC008.

F. Plagioclase-phyric felsic volcanic rock with both phenocrysts and matrix affected by hematized K-feldspar alteration and K-feldspar + quartz + calcite veining. MFC013002B.

Abbreviations: Kfs=K feldspar, act=actinolite, di=diopside, ttn=titanite, ab=albite, hem=hematite, qtz=quartz. Abbreviations after Kretz (1983).

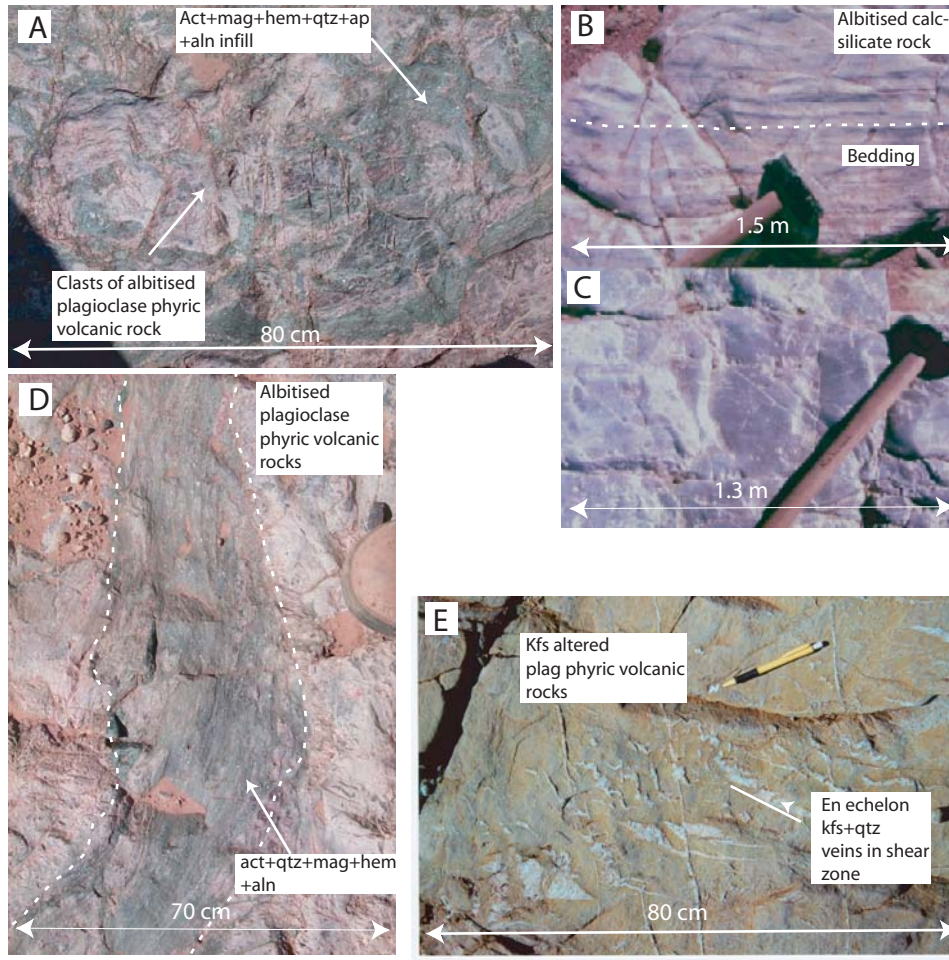


Figure 2.10. Photographs of outcrop from the MFC mapped area showing various metasomatic and structural relationships.

A. Brecciated plagioclase-phyric felsic volcanic rock with actinolite + apatite + titanite + magnetite infill. Clasts are affected by successive stages of albitisation. Photo from river outcrop (see fig. 2.21).

B. Moderately albitised calc-silicate rock. Notice that the relict bedding is still visible.

C. Intensely albitised calc-silicate rock. Notice that the bedding within the rock is completely destroyed by albitisation.

D. Sheared actinolite + magnetite + apatite + titanite vein in an albitised plagioclase-phyric felsic volcanic rock. Photo from river outcrop (see figure 2.21).

E. Plagioclase-phyric felsic volcanic rock affected by hematite K-feldspar alteration and K-feldspar + quartz + calcite veining. Photo from river outcrop (see figure 2.21).

Abbreviations: Kfs=K-feldspar, qtz=quartz, act=actinolite, mag=magnetite, ab=albite, hem=hematite, ap=apatite, aln=allanite. Abbreviations after Kretz (1983).

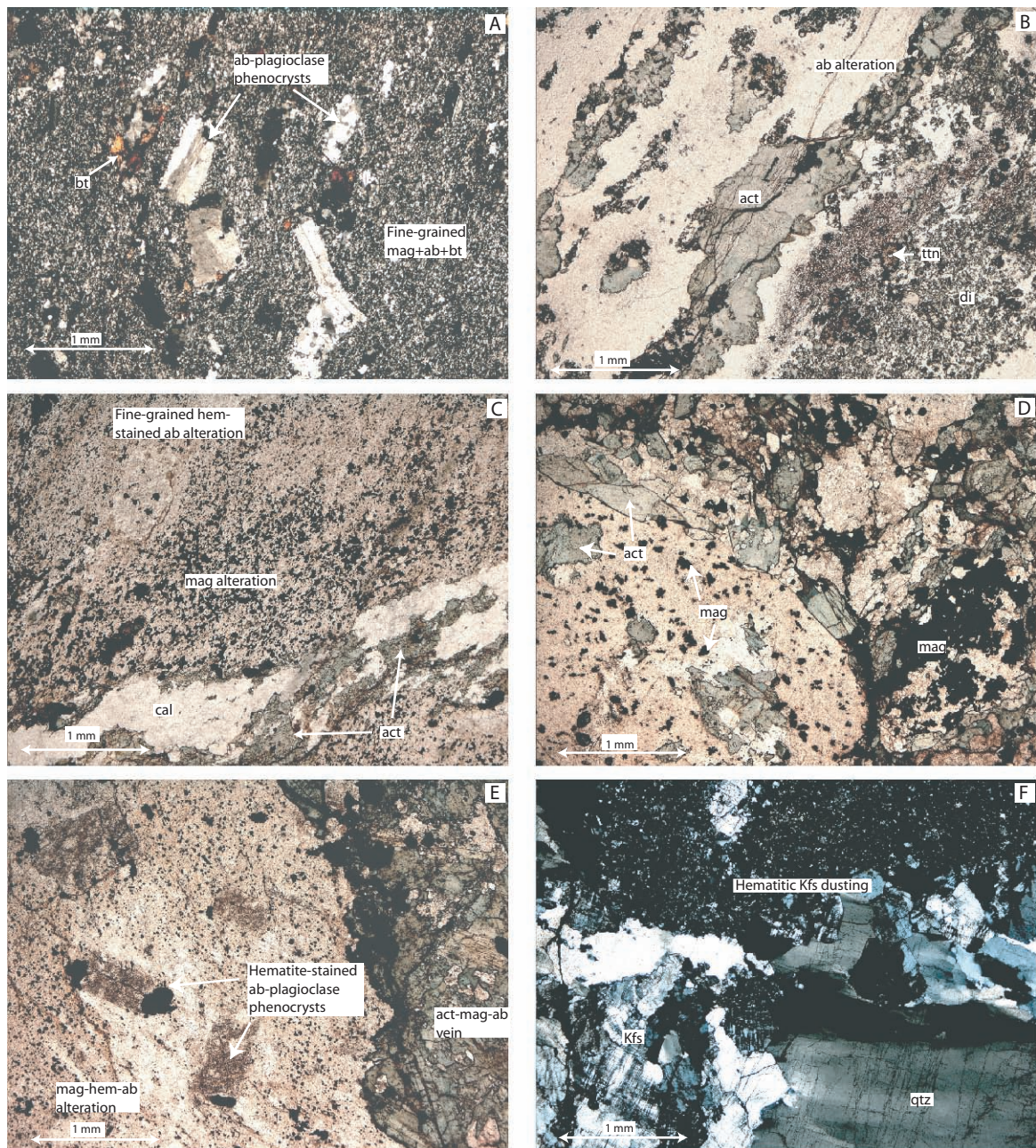


Figure 2.11. Photomicrographs of rock types and alteration styles identified within outcrop at MFC.

A. Albitised felsic volcanic rock with aligned relict plagioclase phenocrysts probably related to primary flow banding (Cross-polarised light: XPL). MFC047.

B. Albitised felsic volcanic rock cut by actinolite + diopside + titanite + albite veining (Plane-polarised light: PPL). MFC008.

C. Hematite-stained albite altered felsic volcanic rock cut by actinolite + calcite vein associated with fine-grained magnetite alteration (PPL). MFC013007A.

D. Brecciated felsic volcanic rock with actinolite + magnetite infill and albite alteration (PPL). Small magnetite grains are also present within the felsic volcanic clasts. MFC012.

E. Felsic volcanic rock cut by actinolite + magnetite + albite vein. Relict plagioclase phenocrysts replaced by hematite-stained K-feldspar alteration. Small magnetite grains within the felsic volcanic rocks are associated with an earlier alteration event (PPL). MFC121.

F. K-feldspar + quartz + calcite vein cutting hematite-stained K-feldspar-altered felsic volcanic rock (XPL). MFC013002B.

Abbreviations: Kfs=K-feldspar, qtz=quartz, act=actinolite, mag=magnetite, ab=albite, hem=hematite, bt=biotite, ttn=titanite, di=diopside. Abbreviations after Kretz (1983).

and could represent either forceful displacement, or flattening of a fabric, around an intrusion.

2.5.2. Mafic metamorphosed rocks

Coarse-grained gabbroic rocks are the dominant rock type identified in drill core from the FC12 prospect, and comprise approximately 85-90 % of the total rock package. They are typically coarse-grained, and contain plagioclase (10-80 %), amphibole (20-30 %), biotite (*ca.*5 %), magnetite (5-7 %), ilmenite (5-7 %), pyrite (0-5 %), orthopyroxene (0-10 %) and clinopyroxene (10-20 %) (Fig. 2.12a and 2.13a). Plagioclase grains vary in size from <5 to 15 mm. Medium-grained gabbroic rocks at FC12 occur as 1 to 5 metre intervals, where contacts between medium- and coarser-grained gabbroic rocks are typically sharp and planar. Medium-grained gabbroic rocks are generally equigranular and contain plagioclase (largely seriticised) (up to 50 %), biotite (*ca.*5 %), clinopyroxene (15-20 %), orthopyroxene (2-20 %), magnetite (2-5 %), ilmenite (2-5 %) and minor pyrite (1-2 %). Clinopyroxene grains are commonly aligned. Felsic igneous rocks commonly cut both medium- and coarse-grained gabbroic rocks (Fig. 2.12b), however, magma mingling between both rock types is rarely observed. Both medium- and coarse-grained gabbroic rocks are affected by progressive stages of alteration including early biotite veining, followed by texturally complex actinolite- and carbonate-rich Na-Ca veins and minor hematite-stained albite alteration.

At FC4NW, mafic igneous rocks metamorphosed to amphibolite facies intrude both metasedimentary and calc-silicate rocks to the north-east in drill holes MFC98052, MFC98053 and MFC98054 (Fig. 2.6). These rocks are dark green to black in colour and exhibit a metamorphic fabric (Fig. 2.8d, e). They are typically composed of hornblende ($Mg/(Mg+Fe) = 0.60$) + biotite + plagioclase and are affected by Na-Ca alteration and later hematite-stained K-feldspar or albite alteration. In outcrop, a N-S-trending diorite dyke appears to post-date all identified hydrothermal events. The rock is dark green to black in colour, and is composed of plagioclase (40-50 %), quartz (10-15 %) and hornblende (30-40 %). Aeromagnetic data highlights the dioritic dyke as a thin N-S trending feature that is up to 20 m across and is poorly exposed at surface (Fig. 2.7).

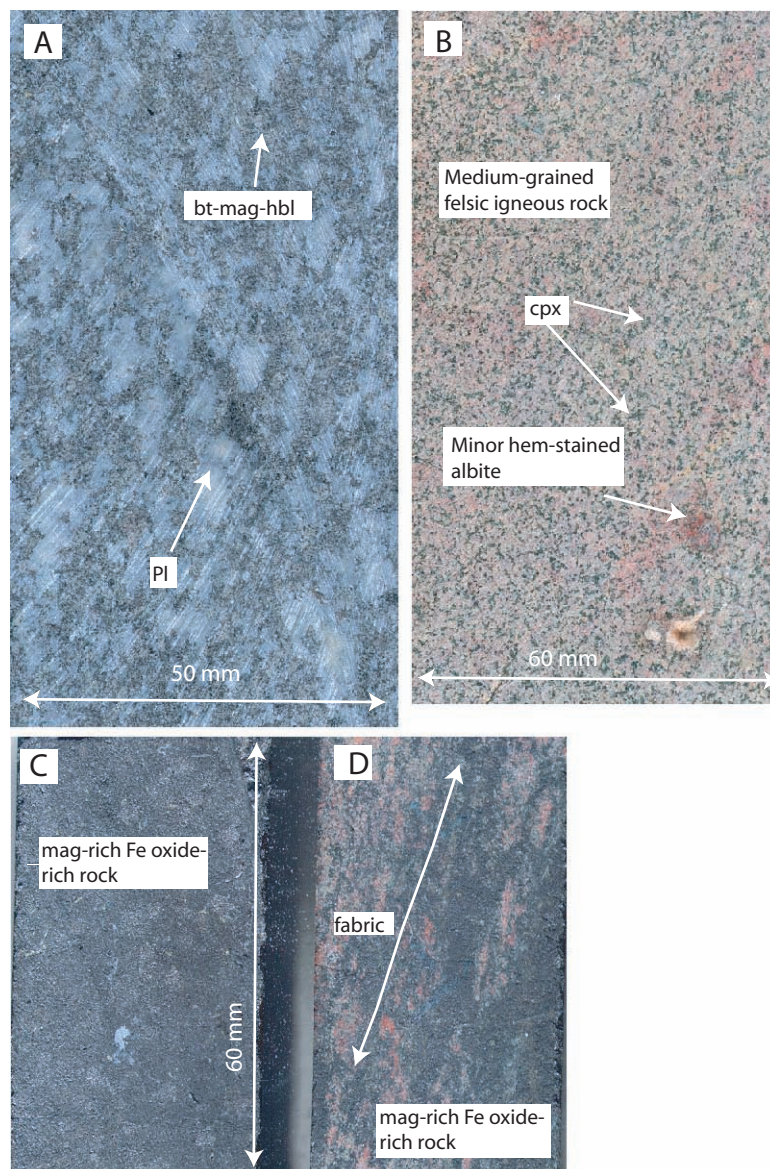


Figure 2.12. Photographs of rock types observed at the FC12 prospect.
A. Coarse-grained tholeiitic gabbro composed of large plagioclase grains as well as magnetite, biotite and hornblende. FTCD1082, 384.5 m.
B. Fine-grained albitised felsic igneous rock affected by later hematite-stained albite alteration. FTCD1087, 263.8 m.
C. Fe oxide-rich 'ironstone' rock with minor biotite. Note Fe oxide-rich rock exhibits a massive texture. FTCD1081, 289.6 m.
D. Fe oxide-rich 'ironstone' rock with minor albite. Note distinct tectonic fabric. FTCD1081, 291 m. Abbreviations: Bt=biotite, mag=magnetite, amp=amphibole, hem=hematite, cpx=clinopyroxene, pl = plagioclase feldspar. Abbreviations after Kretz (1983).

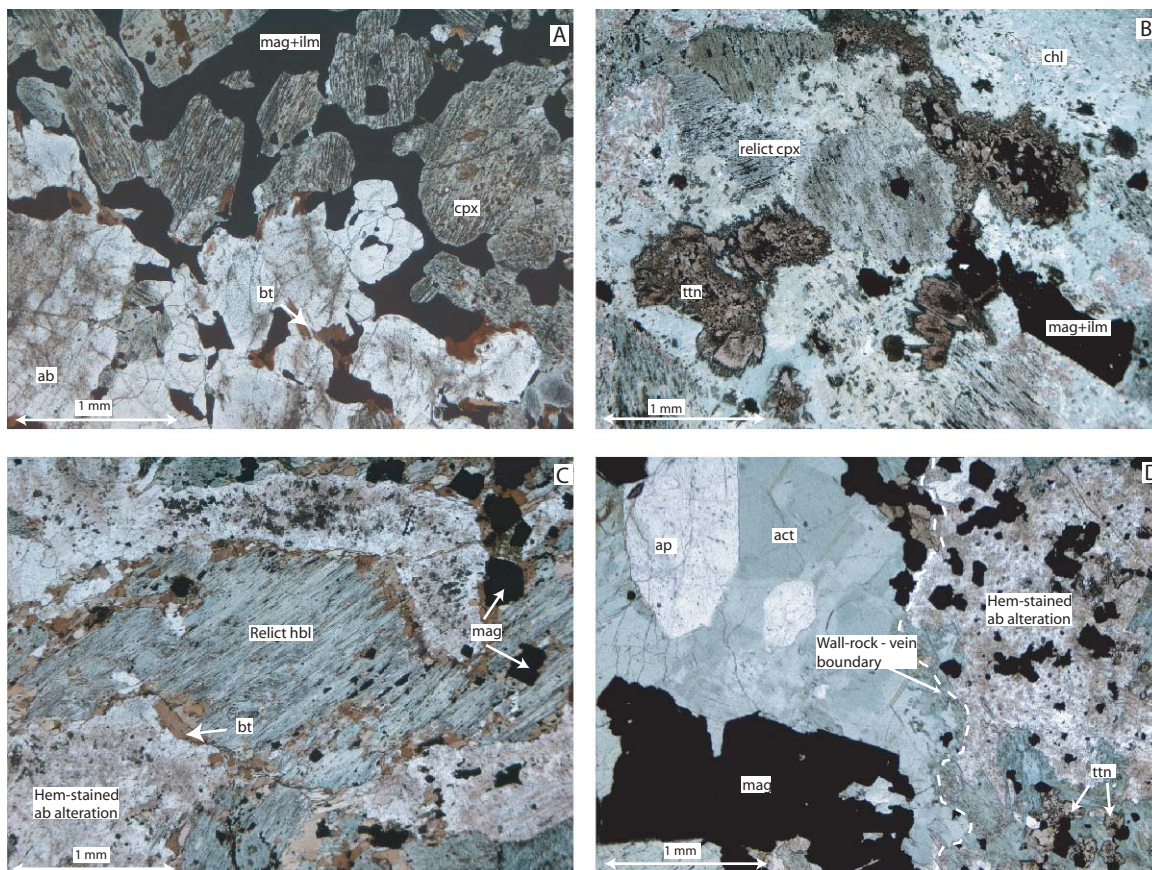


Figure 2.13. Photomicrographs of rock types and alteration styles identified at the FC12 prospect.

A. Coarse-grained gabbroic rock composed of magnetite + ilmenite + clinopyroxene + albite (Plane Polarised Light: PPL). FTCD1087, 371.2 m.

B. Highly-altered, coarse-grained gabbroic rock with the replacement of clinopyroxene by chlorite and ilmenite by titanite. (PPL). FTCD1086, 209.8 m.

C. Gabbroic rock with relict actinolite being replaced by biotite and affected by later hematite-stained albite alteration (PPL). FTCD1085, 101.4 m.

D. Actinolite + apatite + magnetite + calcite + pyrite Na-Ca vein cutting coarse-grained gabbroic rock. Gabbroic rock is affected by later hematite-stained albite alteration (PPL). FTCD1082, 347 m.

Abbreviations: mag=magnetite, ab=albite, hem=hematite, hbl=hornblende, act=actinolite, ilm=illmenite, bt=biotite, cpx=clinopyroxene, ttn=titanite, ap=apatite, py=pyrite, chl=chlorite. Abbreviations after Kretz (1983).

2.5.3. Felsic igneous rocks

Felsic igneous rocks are observed within drill core from the FC4NW and FC12 prospects (Fig. 2.8c, d, e, f and 2.12b), however, they appear to be more common at FC4NW (Fig. 2.5, 2.6). In drill core, intervals of felsic igneous rocks can vary in size from centimetre-scale to <1-10 m thick, are equigranular and are invariably affected by intense albitisation and later hematite-stained K-feldspar and albitic alteration. The typical mineral assemblage of these rocks includes albitic plagioclase (An_{2}) (*ca.*70 %), quartz (*ca.*5-20 %), clinopyroxene (*ca.*10 %) and rare titanite. The mineral assemblage of these rocks closely resembles clinopyroxene-rich Na-Ca alteration assemblages at FC4NW discussed below, inferring a potential genetic link. Rare myrmekitic textures are preserved, and are attributed to either the simultaneous crystallisation of alkali feldspar and quartz, or the replacement of some of the alkali feldspar by quartz (Gribble and Hall, 1992). These felsic igneous rocks are similar in both the FC12 and FC4NW prospects and exhibit many similarities to coarse-grained syenite/quartz syenite intrusions and Na-rich phases of the Mount Margaret intrusion (1530 ± 8 Ma, Page and Sun, 1998), located approximately 12 km northeast of the Ernest Henry mine (Pollard et al., 1998) (Fig. 2.1).

Late-stage pegmatite dykes in the FC4NW prospect commonly cut granitic intrusions (Fig. 2.6, 2.8c). The dykes are coarse-grained (up to 4 mm) and contain variable proportions of quartz and alkali feldspar and are commonly affected by albite alteration. Dykes vary in thickness from 1 to 5 cm wide, and mostly exhibit a finer-grained texture along the margins that may be the result of rapid cooling. Similar dykes elsewhere in the EFB have been interpreted to be associated with the last stages of magma crystallisation within the potassic intrusions of the Williams and Narku Batholiths (Dare, 1995; Tolman, 1998; Mark, 1999). Balloon-textured albite- and quartz-rich magmatic rocks along with infill-supported magmatic-hydrothermal breccias (actinolite, albite and apatite) at the Mount Angelay igneous complex (Mark, 1999) suggest that Na-Ca alteration formed from processes involving a magmatic-hydrothermal transition. While the evidence is not as clear at MFC, the close spatial and temporal relationship between granitic rocks and Na-Ca alteration at FC4NW support a possible genetic relationship between the intrusions and the alteration.

2.5.4. Metasedimentary rocks

Biotite-bearing metapelite

The dominant metasedimentary rock types at the FC4NW prospect are fine-grained, psammitic metasedimentary rocks that contain a relict layering and banding (Fig. 2.6, 2.8a, c, f). This layering and banding is highly variable and difficult to constrain due to alteration. In hand specimen, the rocks have a dark grey to black colour, and individual minerals are largely indistinguishable with a hand lens. Where alteration is minor, minerals observed under the microscope in the metasedimentary rocks include fine- to medium-grained quartz, plagioclase feldspar, biotite, muscovite and magnetite. These rocks commonly exhibit fine granoblastic textures, as well as a locally well-defined fabric in thin section characterised by the alignment of biotite grains. They are typically highly magnetic due to early magnetite alteration. These rocks resemble similar biotite-muscovite-bearing metasedimentary rocks identified by Mark et al (1999) within the term lease around the Ernest Henry deposit, and may be of similar affinity.

Calc-silicate rocks

Skarn-like calc-silicate rocks are observed in outcrop to the north of the MFC hill and within drill core from the FC4NW prospect, and in both cases are interpreted to be part of the Corella Formation (1780-1725 Ma) (Fig. 2.9a). No pristine calc-silicate rocks were identified, and those detected are typically fine-grained (<100 µm) and exhibit an apple green colour in fresh rock. In thin section, their mineral assemblage includes diopside (80-85%) with minor quartz, albite, apatite, biotite and titanite. Deformed calc-silicate rocks display complex fold and shear structures. Relict bedding is commonly observed, and where albitised, alteration is most intense along these bedding planes.

2.6. ALTERATION

The aim of this section is to describe the paragenetic history observed in outcrop and at the FC4NW and FC12 prospects at MFC. Electron probe microanalysis was performed on amphibole, clinopyroxene, feldspar and biotite from all three areas in addition to GADDS (General Area Diffraction Detection System) for mineral identification. Representative results of electron probe data are presented in table 2.1, while all results are presented in appendix 2.

The alteration observed at MFC (Fig. 2.14) can be broken down into the following sequential categories according to their mineral assemblage and texture:

1. Albitisation
2. Na±Ca alteration: main phase of sulphide mineralisation at FC4NW and FC12
3. Fe oxide-rich metasomatism
4. Red-rock alteration: K-feldspar and / or hematite-stained albite alteration

2.6.1. Albitisation

Albite alteration represents the earliest metasomatic event observed throughout the MFC exploration lease (Fig. 2.14). It is dominant in the NE and SW quadrants of the mapped area of outcrop (Fig. 2.7), whereas at the FC4NW prospect, albitisation is most intense toward the southwest (Fig. 2.6). In hand specimen, it occurs with a pale white, fine-grained, sugary texture that, depending on intensity, may destroy much of the primary texture of the rock (Fig. 2.10b, c). In thin section, albite alteration preferentially replaces the more calcic plagioclase in felsic volcanic rocks prior to affecting the other minerals. Typically all rock types are affected, although albite alteration appears to be locally more pronounced in the metasedimentary and calc-silicate rocks where it commonly utilises bedding planes and previous tectonic fabrics (Fig. 2.15a). Albitic plagioclase commonly has below detection limit CaO ($An_{\leq 2}$), common to many Na and Na-Ca assemblages throughout the Cloncurry district (*cf.* Mark, 1998b). Albite was also identified using GADDS.

2.6.2. Na-Ca alteration

FC12

A range of different styles of Na-Ca alteration were observed in the three areas of study, where the FC4NW and FC12 prospects contain the clearest examples. Of particular note is Na-Ca veining at FC12 that exhibits distinctive textures and mineralogy. These veins range from *ca.* 1 to 10 cm in width and trend at a high angle to the drill core axis. Na-Ca veining is more abundant to the northern part of the prospect, with spacing between veins varying from *ca.* 10 cm to 100 cm in the north to several metres in the south (Fig. 2.5b). They also rarely occur as localised clast-supported breccia zones. These veins are zoned, and always show adjacent wall-rock alteration as follows:

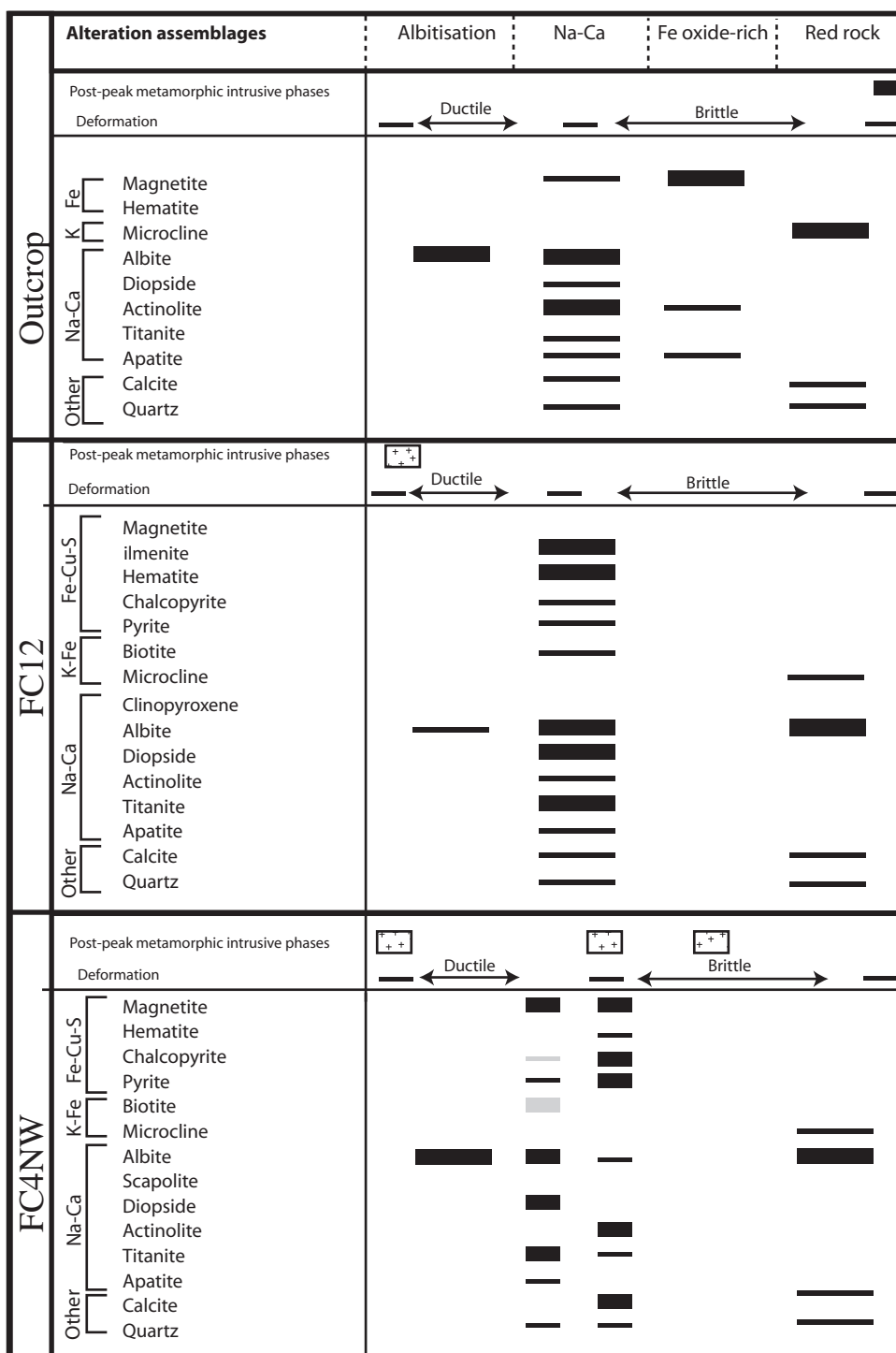


Figure 2.14. Paragenesis of major alteration phases at the FC12 and FC4NW prospects and MFC outcrop. Their relationship to post-peak metamorphic intrusive rocks and styles of deformation is also shown. Note minerals represented by grey bars in the FC4NW prospect occur in association with coarse-grained biotite alteration only.

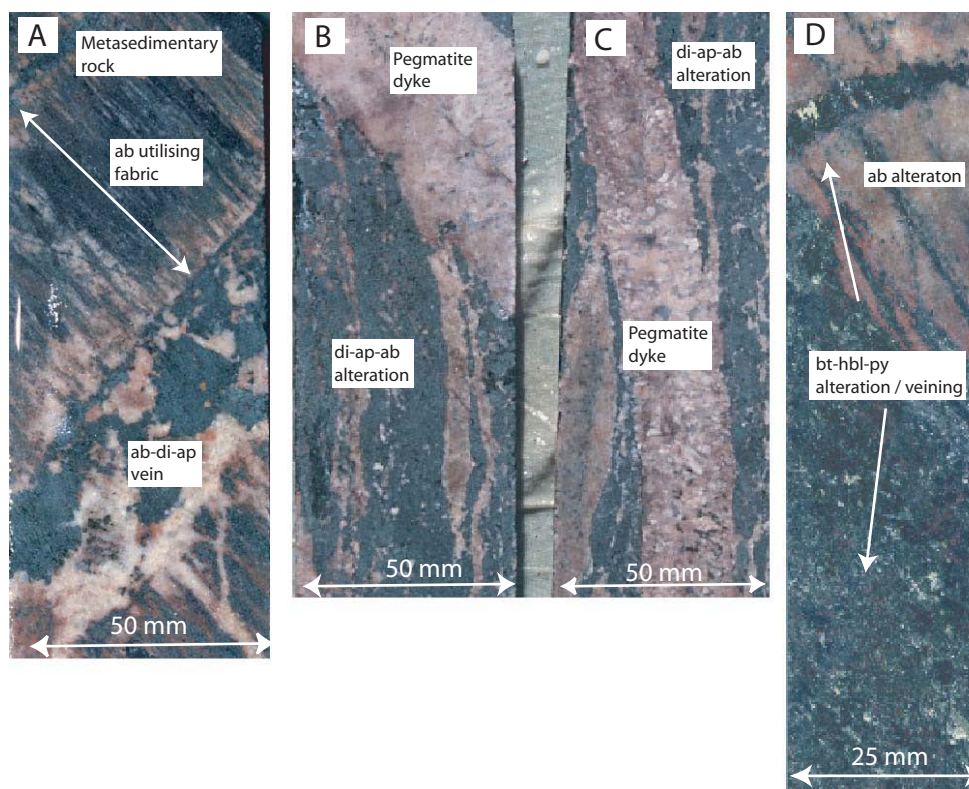


Figure 2.15. Hydrothermal alteration phases observed at the FC4NW prospect.
 A Metasedimentary rock cut by diopside + apatite + albite veining and alteration. MFC98052, 250 m.
 B. Intense clinopyroxene-rich Na-Ca alteration cut by coarse-grained pegmatite dykes. Relict felsic igneous rock overprinted by clinopyroxene-rich Na-Ca alteration. MFC98052, 269 m.
 C. Intense clinopyroxene-rich Na-Ca alteration cut by coarse-grained pegmatite dykes. Relict felsic igneous rock overprinted by clinopyroxene-rich Na-Ca alteration. MFC98052, 269 m.
 D. Albitised metasedimentary rock cut by biotite-amphibole alteration and veining. Biotite within these veins contain between 1 to 1.5 wt% Ti. MFC98051, 160.5 m.
 Abbreviations: di=diopside, ab=albite, ap=apatite, hbl=hornblende, bt=biotite, py=pyrite. Abbreviations after Kretz (1983).

- Alteration halo: chlorite + titanite replacing ilmenite + magnetite + actinolite + albite (hematised due to later red rock alteration) ± pyrite ± biotite ± epidote (Fig. 2.13b, c, d, 2.16a, 2.17).
- Outer portion of vein adjacent to wallrocks: magnetite + actinolite + albite + titanite ± pyrite ± chalcopyrite ± apatite (Fig. 2.13d, 2.16a,f, 2.17).
- Central part of vein: calcite + albite ± specular hematite ± pyrite ± chalcopyrite (Fig. 2.16b, c, d, 2.17).

Actinolites at the vein edges typically have Mg No. of 60 to 75 (Mg No. = $(\text{Mg}/(\text{Mg}+\text{Fe})) * 100$), whereas actinolite within the alteration halos typically is more Mg-rich (Mg No.: 55 to 70). Rare ferro-actinolite (Mg No.: 42-48) was found at the edge of some veins and is characterised by an intense green colour under the microscope in plane-polarised light (PPL). The alteration halo associated with these veins range in size from mm to cm scale, and commonly exhibits a green colouration due to the high proportion of chlorite. The formation of hematite within the centre of these veins and magnetite at the margin may reflect the fluid becoming more oxidised and/or cooling over time, although the small vein size suggests that a decrease in temperature was a less likely cause than f_{O_2} (Fig. 2.16e, f, 2.17b, c). Chalcopyrite occurs as infill in the centre of the veins, apparently in textural equilibrium with specular hematite, calcite, pyrite and albite ($\text{An}_{\leq 2}$) and represents the only Cu-bearing mineral at FC12 (Fig. 2.16b). This is illustrated by figure 2.5b and c, where Na-Ca veining and chalcopyrite distribution overlap. Cu grade within the FC12 prospect rarely exceeds 3000 ppm, although a one metre-long interval exhibits Cu up to 2 wt % (FTCD 1082, 357.7-359.8 m).

FC4NW

Na-Ca alteration at FC4NW occurs as two mineralogically distinct phases: a clinopyroxene-rich phase (Fig. 2.15a, b, c) and an amphibole-rich phase (Fig. 2.18c, d). Separating these two alteration phases is a biotite-amphibole association, the timing of which is commonly difficult to separate from clinopyroxene-rich Na-Ca alteration but is interpreted to be later (see below). The mineral assemblage of each of these alteration phases includes:

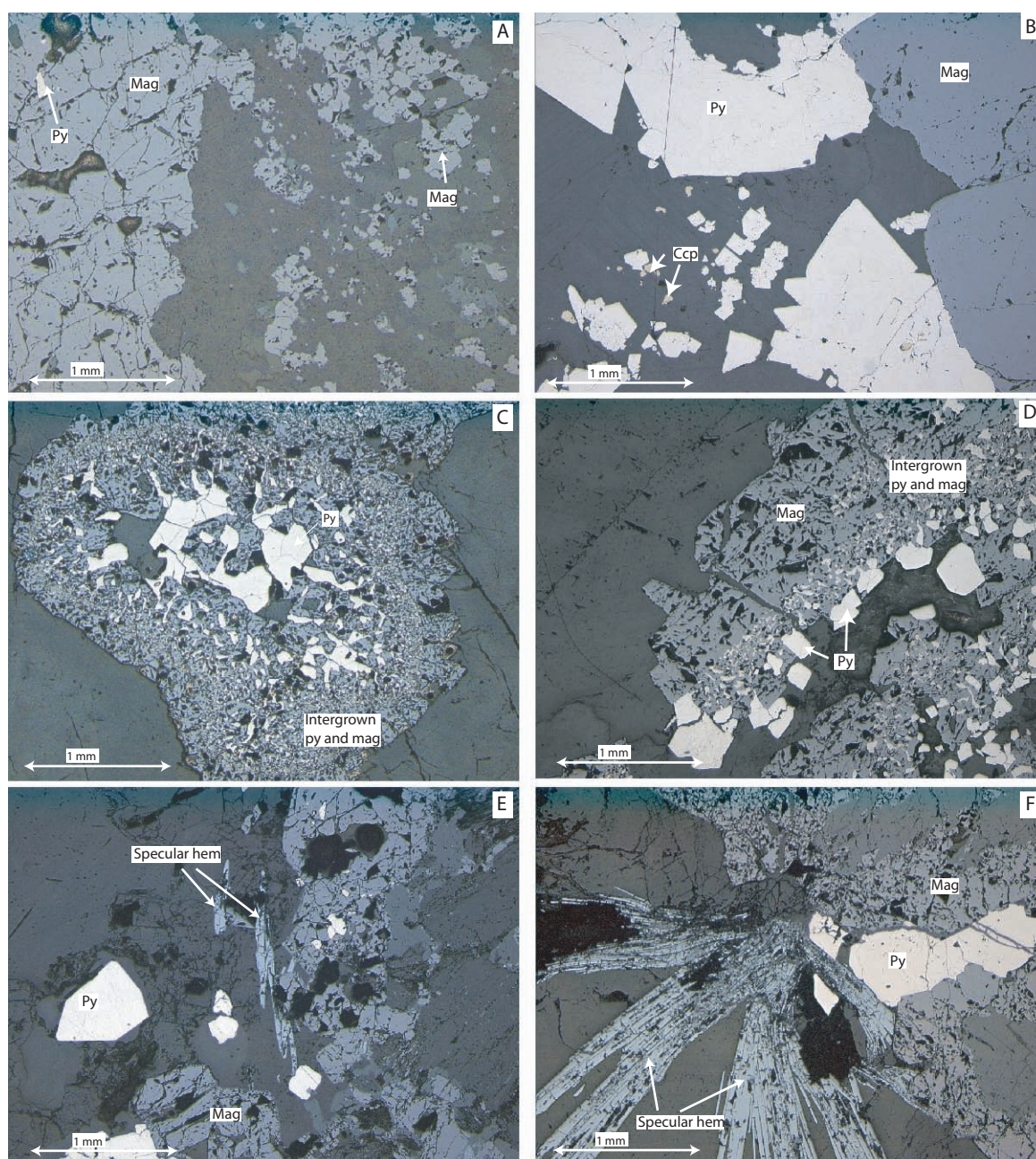


Figure 2.16. Photomicrographs of sulphides and oxides observed within the FC12 prospect.

A. Na-Ca vein in gabbroic rock with magnetite + pyrite at vein/wall rock boundary and interstitial magnetite associated with coarse-grained gabbro (Reflected light). FTCD1082, 347 m.

B. Large pyrite and magnetite grains in a Na-Ca vein with minor chalcopyrite. Note small chalcopyrite inclusions in pyrite grains (Reflected light). FTCD1081, 356.8 m.

C. Complex intergrown pyrite and magnetite grains associated with Na-Ca veining in a coarse-grained gabbro (Reflected light). FTCD1086, 206 m.

D. Complex intergrown pyrite + magnetite grains associated with Na-Ca veining in a coarse-grained gabbro. Note large pyrite grains on the edge of the large magnetite grains (Reflected light). FTCD1081, 431 m.

E. Na-Ca vein with magnetite + pyrite at wall-rock/vein boundary and specular hematite + pyrite + chalcopyrite in the centre of the vein (Reflected light). FTCD1087, 201 m.

F. Na-Ca vein with mag+py at wall-rock/vein boundary and specular hematite + pyrite + chalcopyrite on the vein-wall rock boundary growing towards the centre of the vein. (Reflected light). FTCD1087, 187 m.

Abbreviations: mag=magnetite, py=pyrite, ccp=chalcopyrite, hem=hematite. Abbreviations after Kretz (1983).

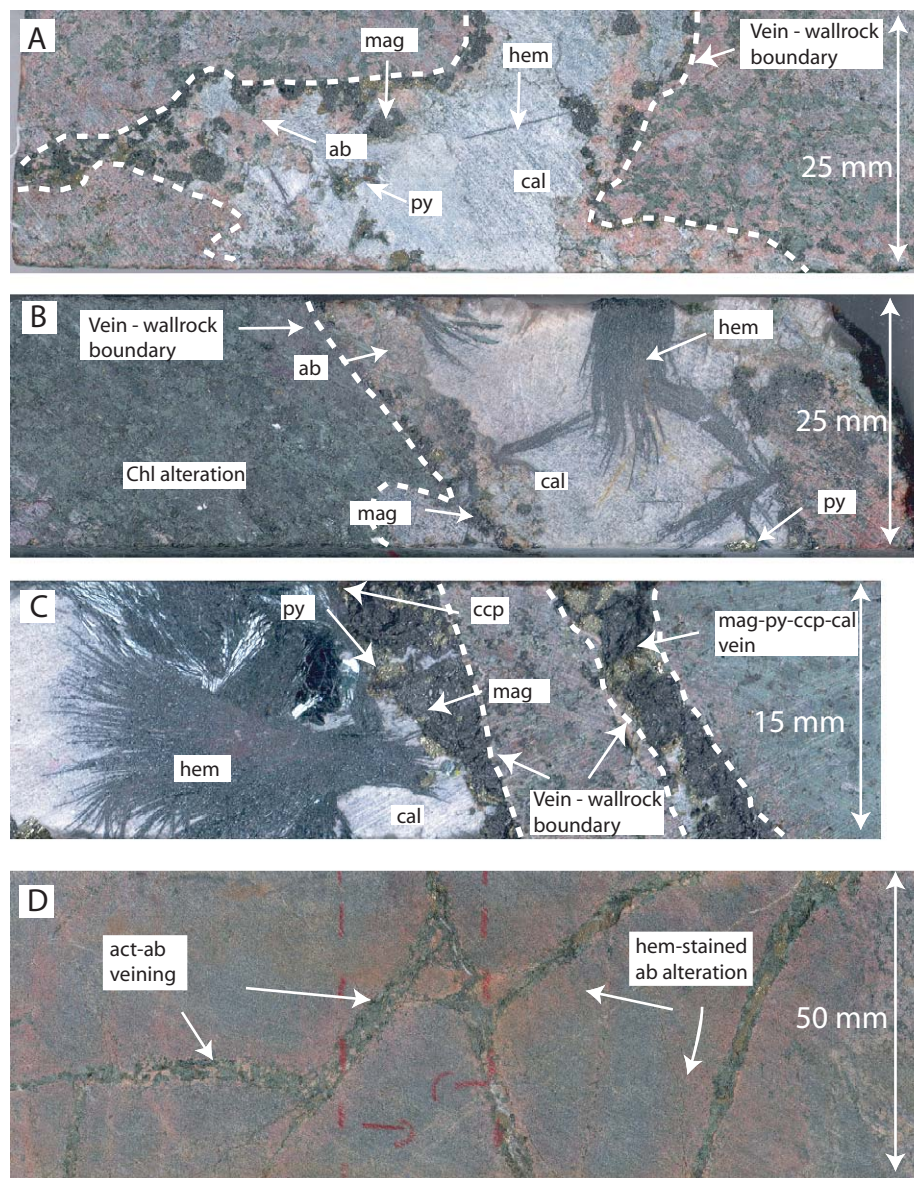


Figure 2.17. Hydrothermal alteration phases observed at the FC 12 prospect.
 A. Coarse-grained gabbroic rock cut by magnetite + pyrite + chalcocopyrite + hematite + calcite + albite vein. Note that magnetite and albite occurs close to the vein-wall rock boundary while calcite and hematite occurs in the centre of the vein. FTCD1087, 183 m.
 B. Medium-grained gabbroic rock cut by magnetite + albite + calcite + hematite + pyrite vein. Large specular hematite is commonly observed to grow towards the centre of the vein from the vein-wall rock boundary. FTCD1087, 203.2 m.
 C. Texturally complex Na-Ca veining containing magnetite + albite + actinolite on the wall-rock-vein margin and calcite + specular hematite + pyrite + chalcocopyrite in the central part of the vein. FTCD1087, 204 m.
 D. Fine grained dioritic rock cut by actinolite + calcite + magnetite + albite veins, which are later effected by hematite-stained albite alteration. FTCD1087, 192.2 m.
 Abbreviations: act=actinolite, ab=albite, hem=hematite, mag=magnetite, py=pyrite, cal=calcite, chl=chlorite, ccp=chalcocopyrite. Abbreviations after Kretz (1983).

Figure 2.18. Hydrothermal alteration phases observed in the FC4NW prospect.

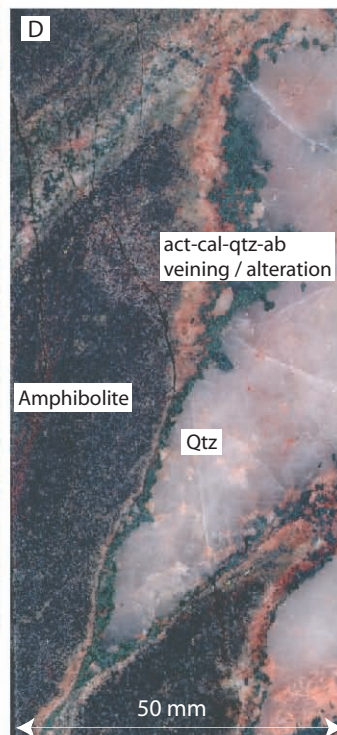
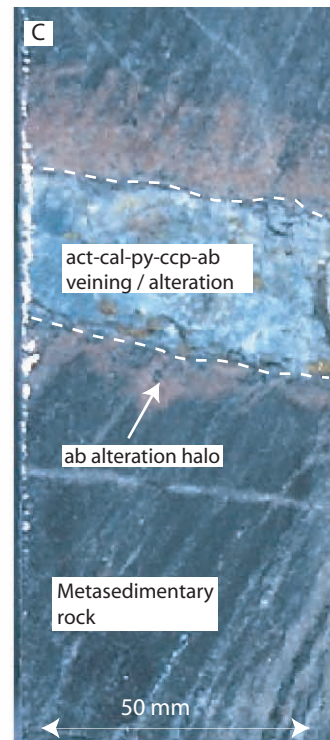
A. Fe oxide-rich 'ironstone' metasomatism altering metasedimentary rock. Magnetite associated with pyrite, diopside and minor chalcopyrite. MFC99090, 254.8 m.

B. Fe oxide-rich 'ironstone' metasomatism. Magnetite associated with clinopyroxene and pyrite and is overprinted by actinolite + magnetite + chalcopyrite + pyrite + calcite + quartz infill and alteration. MFC97027, 81.9 m.

C. Dark, fine-grained metasedimentary rock cut by actinolite + chalcopyrite + pyrite + calcite veining and alteration. Note albite alteration utilising relict fabric and bedding planes. MFC98-51, 159.8 m.

D. Dark, fine-grained amphibolite rock cut by actinolite + calcite + quartz + albite veining and alteration. MFC99092, 187 m.

Abbreviations: act=actinolite, ab=albite, mag=magnetite, py=pyrite, cal=calcite, qtz=quartz, ccp=chalcopyrite, ttn=titanite, ap=apatite, hd=hedenbergite. Abbreviations after Kretz (1983).



- *Clinopyroxene-rich association:* Diopside + titanite + albite ± magnetite ± apatite ± pyrite ± calcite ± tourmaline (Fig. 2.19b, c, d, e).
- *Biotite-amphibole association:* Biotite + hornblende ± pyrite (Fig. 2.15d).
- *Amphibole-rich association:* actinolite + calcite + magnetite + albite ± pyrite ± chalcopyrite ± quartz ± titanite ± hematite (Fig. 2.19d, e).

Clinopyroxene-rich Na-Ca alteration occurs both as a pervasive alteration and a brittle-ductile veining system (Fig. 2.15a, b, c), affecting all rock types and varying in size from <2 mm to several meters in scale. Diopside has a Mg No. 55-70, while plagioclase is albitic ($An_{\leq 2}$). Albitisation commonly accompanies clinopyroxene alteration and is most pronounced in the metasedimentary rocks where the alteration utilises the primary bedding and tectonic fabric (Fig. 2.15a). Clinopyroxene-rich Na-Ca alteration is overprinted by amphibole-rich Na-Ca alteration and hematized K-feldspar / albite alteration, and is interpreted to be temporally related to Fe oxide metasomatism at FC4NW (discussed below).

Coarse-grained biotite-amphibole alteration is observed in both metasedimentary rocks and amphibolite (Fig. 2.6f), and is commonly associated with magnesian hornblende (Mg No.: 64) ± pyrite (Fig. 2.19a). Biotite-amphibole alteration predominantly occurs as a locally intense replacement of the original host rock, but forms thin veins between 1 and 2 cm wide (Fig. 2.15d). The biotite (Mg No.: ~55) typically exhibits a dark brown colour and is Ti-rich (~2.5 wt %) suggesting that it may have been produced from high temperature fluids. Although the timing of this alteration is difficult to constrain precisely, it may be related to the clinopyroxene-rich alteration phase (Fig. 2.14, 2.6f, h). No overprinting relationships were observed between biotite-amphibole and clinopyroxene-rich Na-Ca alteration, although both are cut by the later amphibole-rich Na-Ca and hematized K-feldspar / albite alteration (described below).

Amphibole-rich Na-Ca alteration at FC4NW closely resembles the mineralogy of Na-Ca alteration at FC12 described above (Fig. 2.18c, d), except chlorite was not observed around Na-Ca veins at FC4NW. Amphibole-rich Na-Ca alteration is typically associated with brittle veining networks and breccia zones, where localised displacement of host-rocks along these veins is commonly observed (Fig. 2.8f).

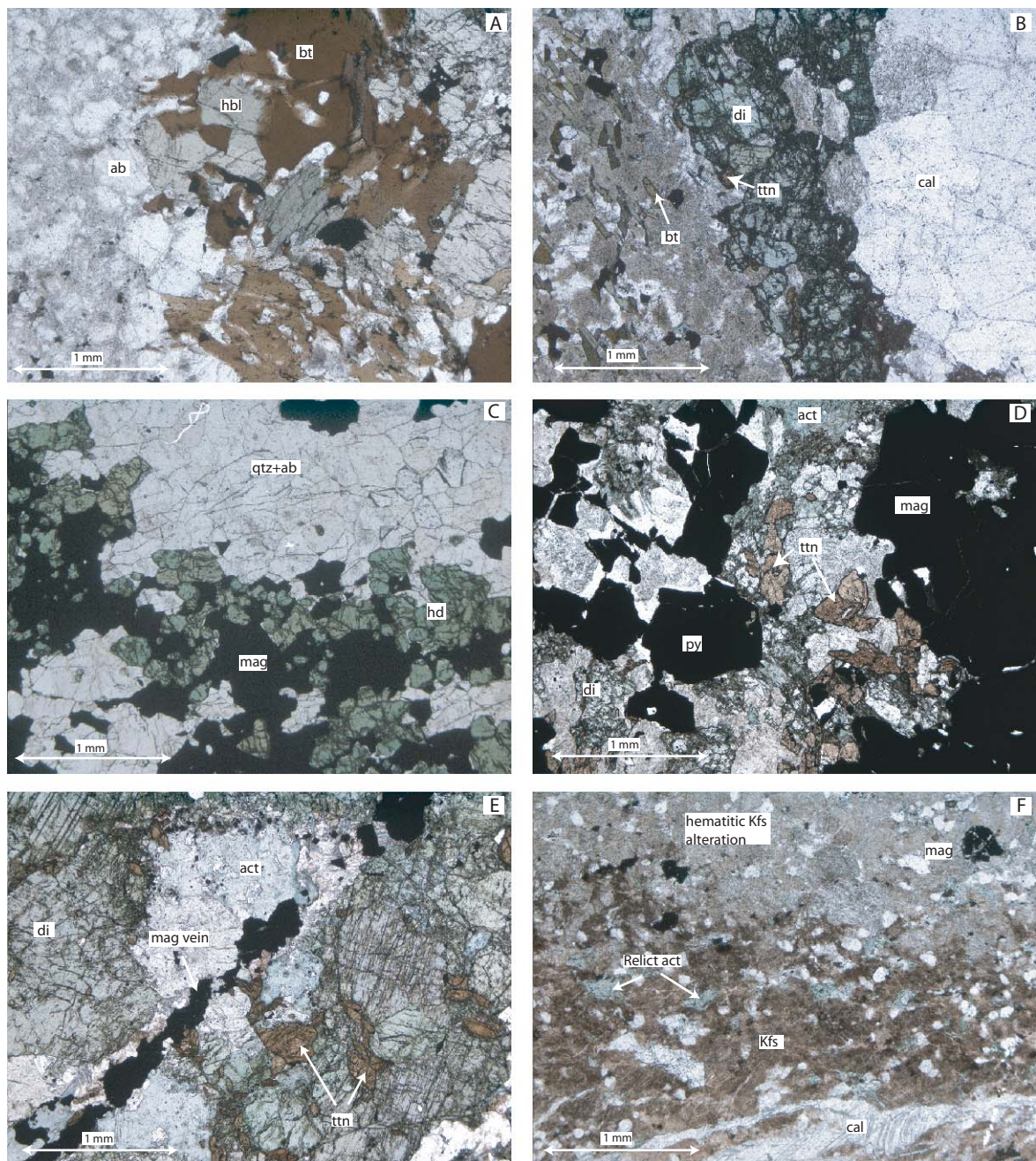


Figure 2.19. Photomicrographs of rock types and alteration phases identified at the FC4NW prospect.

A. Biotite + hornblende + albite vein cutting an albitised metasedimentary rock. MFC98051, 160.5 m.

B. Clinopyroxene-rich Na-Ca vein cutting a biotite-bearing metasedimentary rock. Notice diopside + titanite at wall-rock/vein boundary and calcite within centre of vein. MFC99092, 189 m.

C. Hedenbergite + magnetite alteration (ironstone) overprinting albitised rock. MFC98051, 161.3 m.

D. Fe oxide-rich rock associated with diopside + magnetite + titanite alteration overprinted by actinolite + pyrite + minor chalcopyrite alteration/infill. MFC99090, 254.8 m.

E. Diopside + titanite + albite alteration cut by thin actinolite + magnetite veining/alteration. MFC99091, 224 m.

F. Felsic volcanic rock cut by calcite + hematized K-feldspar + quartz veining and alteration. MFC99090, 176.8 m.

Abbreviations: Kfs=K-feldspar, hbl=hornblende, py=pyrite, qtz=quartz, act=actinolite, mag=magnetite, ab=albite, bt=biotite, ttn=titanite, di=diopside, hd=hedenbergite, cal=calcite. Abbreviations after Kretz (1983).

Actinolite (Mg No.: 50-70) is frequently observed as a replacement of earlier hydrothermal diopside (Fig. 2.19d). Rare ferro-actinolite was also found in some veins (Mg No.: 38-49). The amphibole-rich alteration assemblage at FC4NW is interpreted to be the major sink for Cu mineralisation. This interpretation is supported by the similar spatial distribution patterns of amphibole-rich Na-Ca alteration, chalcopyrite and pyrite shown in figures 2.6n, o and p. Cu values of up to 0.7 wt % is recorded at FC4NW (MFC99090D 260-262 m).

Figures 2.6j and p show that the clinopyroxene-rich alteration phase is more pervasive towards the north of the drill hole transect, while the amphibole-rich phase is more pervasive towards the south. This observation may be due to a number of factors including variation in temperature, pressure, fluid chemistry and/or rock type. The temporal relationship between clinopyroxene-rich and amphibole-rich Na-Ca alteration (Fig. 2.14) is further emphasised by coarse-grained pegmatite dykes. These dykes commonly overprint clinopyroxene-rich alteration (Fig. 2.15b, c), and are in turn cut by amphibole-rich alteration. Although there are a number of factors that may have contributed to a change from clinopyroxene- to amphibole-rich alteration, a decreasing temperature gradient or changes in H₂O:CO₂ ratio provide the most plausible explanations (c.f. de Jong and Williams, 1995). Aeromagnetic data indicate that there are numerous intrusions surrounding the FC4NW prospect (Fig. 2.4), however at this scale, their apparent distribution is not consistent with the observed alteration zonation. Figure 2.6a shows two larger felsic igneous dykes to the NE, whereas felsic igneous dykes to the south are relatively small, which may mean that a granitic intrusion is located very close to the NE quadrant of FC4NW. Evidence for a down-temperature gradient with time is also supported by the transition from ductile (clinopyroxene-rich) to brittle (amphibole-rich) deformation and the presence of quartz and calcite associated with amphibole-rich alteration, where qtz+cc+act represents a lower T and/or higher XCO₂ equivalent of cpx (Fig. 2.18d).

Outcrop

In outcrop, breccia zones range from irregular shaped crackle breccias (Fig. 2.20a) to intensely milled, matrix-supported breccia zones with highly variable clast sizes (Fig. 2.10a), where the matrix is composed of actinolite (80-90 %) with the Mg No. at 63- to 65, apatite (up to 5 %), allanite (ca. 1-2 %), and minor quartz and albitic plagioclase

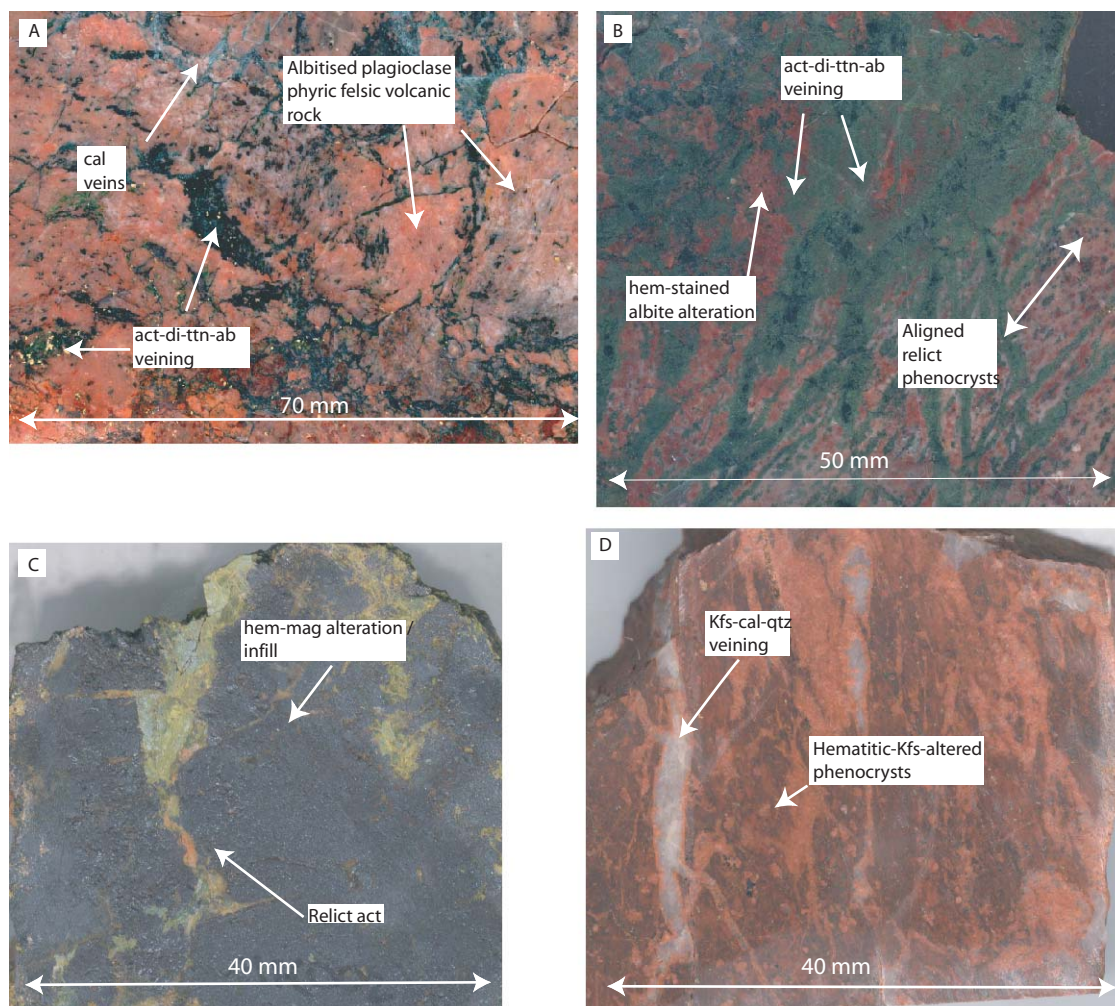


Figure 2.20. Hydrothermal alteration phases observed in outcrop at MFC.

A. Crackle breccia - clasts are intensely albitized felsic volcanic rock. Relict phenocrysts can still be observed. Matrix of the breccia contains actinolite + diopside + titanite + albite. Brecciation is overprinted by late-stage carbonate-quartz veins. MFC143.

B. Plagioclase-phyric felsic volcanic rock intensely altered and brecciated by actinolite + diopside + albite + albite veining and alteration. Note the alignment of altered phenocrysts that may represent original flow banding. MFC051.

C. Fe oxide-rich 'ironstone' containing hematite, magnetite, amphibole and fine-grained apatite. MFC002.

D. Plagioclase-phyric felsic volcanic rock affected by hematite-stained K-feldspar alteration and K-feldspar + quartz + calcite veining. Relict phenocrysts can still be identified in the felsic volcanic rock. MFC013002B.

Abbreviations: act=actinolite, di=diopside, ap=apatite, hem=hematite, mt=magnetite, kfs=K-feldspar, qtz=quartz, cal=calcite, ttn=titanite, ab=albite. Abbreviations after Kretz (1983).

(An₂). Some of the clasts exhibit evidence of multiple brecciation, whereby clasts contain both fragments of previously brecciated rock and earlier Na-Ca alteration. Milled breccia zones exhibit moderate rotation and rounding of locally-derived clasts. Fine-grained magnetite (150-200 µm) commonly occurs as an alteration halo surrounding Na-Ca veins and fractures (Fig. 2.11c). The proportion of magnetite typically decreases away from these fractures and breccia zones. Na-Ca alteration commonly occurs along lithological contacts and intensely brecciated zones in outcrop, and is inferred to be developed due to the competency contrasts between metavolcanic and calc-silicate rocks (c.f. Marshall, 2003). Clasts of both rock types are observed where there are multiple stages of brecciation. However, away from the lithological boundaries, relict layering is still visible within the calc-silicate rocks, defining complex fold patterns, as opposed to the more brittle behaviour of the albitised volcanic rocks.

A strong regional structural control on Na-Ca alteration is inferred from the spatial association between Na-Ca distribution and two NNW-SSE-trending faults (interpreted from aeromagnetic data; Fig. 2.7). One outcrop in particular provides a good example of the structural control on Na-Ca alteration and is situated to the northwest of the mapped area (Fig. 2.7; Fig. 2.21). Only small patches of outcrop appear to be unaffected by Na-Ca alteration (Fig. 2.21). Figure 2.21 shows a 5 m wide breccia sheet trending NNW-SSE that divides the outcrop into rocks affected by Na-Ca alteration and rocks affected by later-stage K-feldspar alteration (discussed below). One possible interpretation for the sharp change in alteration styles is the presence of a large-scale shear zone, which may have displaced rocks affected by both stages. This is supported by the two NNW-SSE-trending faults interpreted from aeromagnetic data, similar to the orientation of the breccia pipe and smaller Na-Ca veins throughout the area (Fig. 2.7). The distribution of alteration superimposed on the aeromagnetic data suggests a component of dextral movement along the fault (Fig. 2.7).

2.6.3. Fe oxide-rich metasomatism

Two Fe oxide-rich 'ironstone' formations are located towards the southern and eastern parts of the mapped area of outcrop (Fig. 2.7). Fe oxide-rich rocks are situated in a pit of old workings, and are exposed in two of the pit walls (Fig. 2.22). Partly albitised quartz-feldspar phyric volcanic rock is the other dominant rock type, with Fe oxide-rich

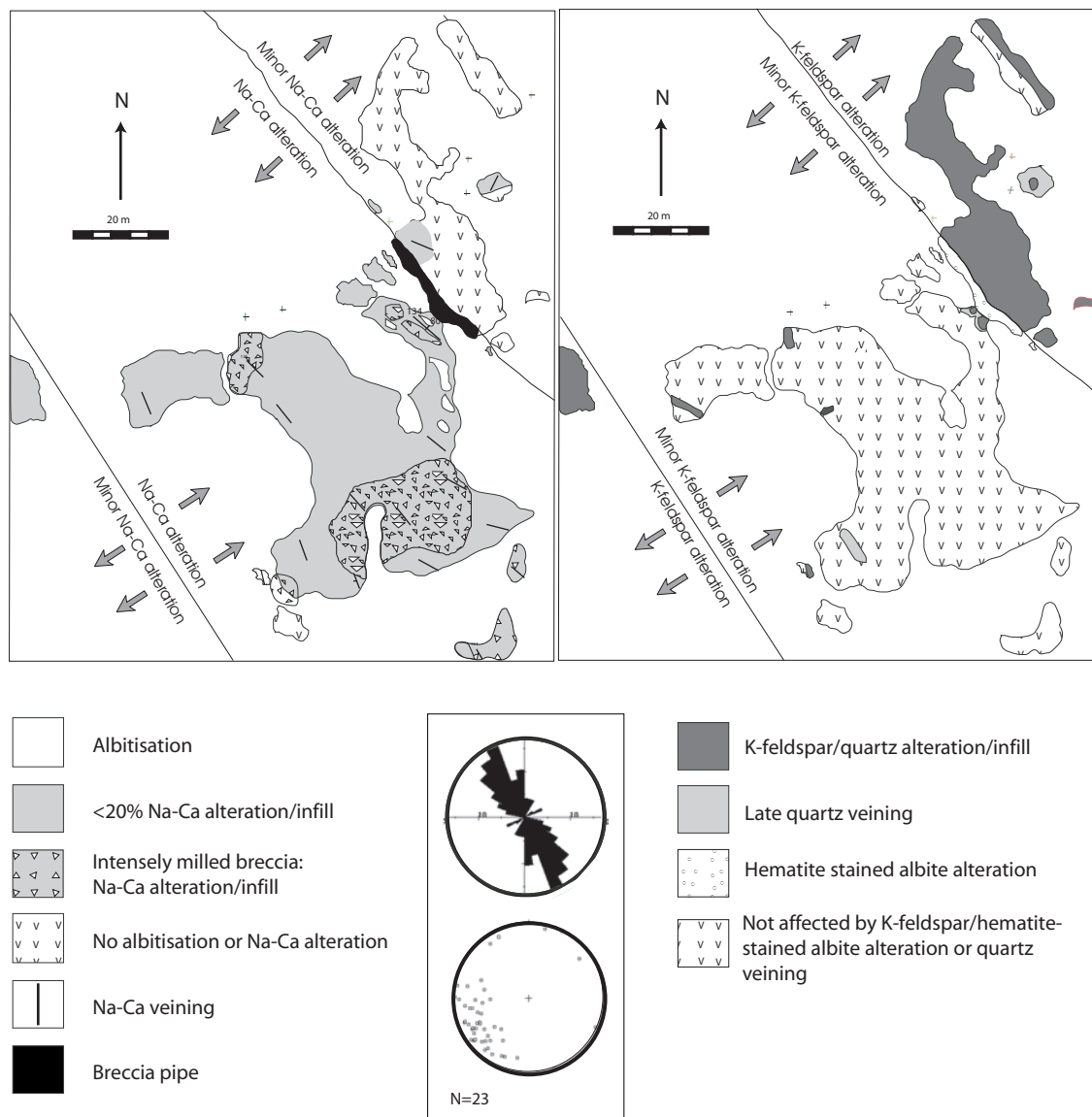


Figure 2.21. Map of large outcrop along the Cloncurry River (see figure 2.7 for location) showing the distribution of Na-Ca alteration and hematised K-feldspar/albite alteration within felsic volcanic rocks. Note the sharp change from Na-Ca to K alteration separated by an intensely milled breccia pipe. This is interpreted to represent a shear zone oriented NW to SE. This interpretation is supported by two faults of similar orientation identified from geophysics (Fig. 2.7).

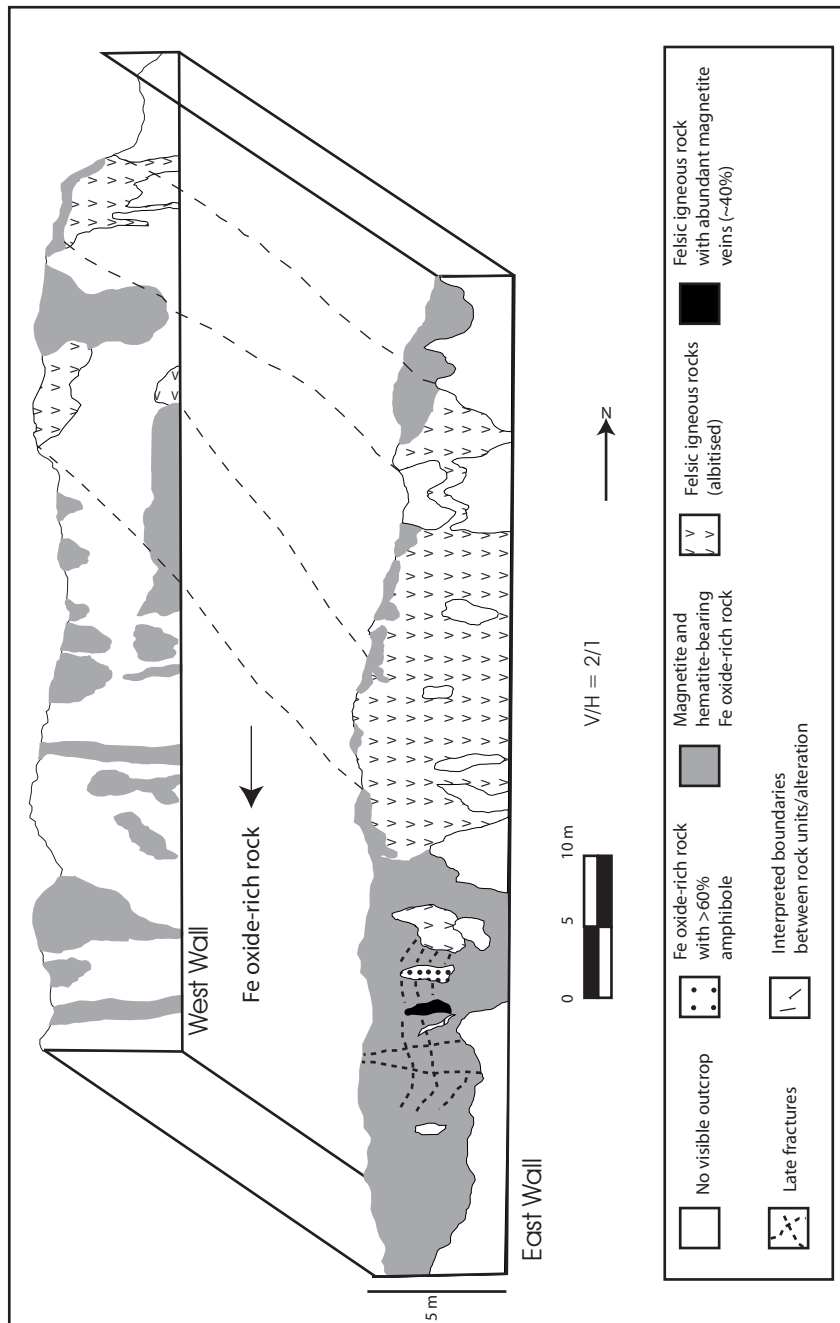


Figure 2.22. Box diagram of variably albitised felsic volcanic rocks and Fe oxide-rich rocks in outcrop located approximately 10 km southwest of the Ernest Henry mine (see figure 2.7 for location). Note sharp contacts between the massive Fe oxide-rich rocks and felsic volcanic rocks.

units lying immediately adjacent to these. The contacts between these two units are sharp. Upon closer inspection, however, small veinlets of hematite and magnetite (1-5 mm) are observed cutting albitised volcanic rocks. Strong weathering of the pit wall hampers any further interpretation of the sharp contacts. Fresher samples of Fe oxide-rich rocks are found as float between the two pit walls. Textures within these fresh samples indicate that the original rock may have been brecciated, with subsequent infill by magnetite and hematite. Clasts are angular suggesting little reworking. It is therefore likely that these Fe-oxide-rich rocks represent breccia pipes within previously albitised volcanic rocks (investigated further in chapter 5).

In thin section, the Fe oxide-rich rocks are dominated by hematite and magnetite, although some of the hematite may be a product of surficial weathering processes. The timing of this metasomatic event is not clear, however, the presence of amphibole (2-3 %) and apatite (2-3 %) associated with hematite and magnetite suggests that it may have a similar timing to Na-Ca alteration observed elsewhere (Fig. 2.20c). A clast containing up to 60 % of weathered amphibole is observed within the Fe oxide-rich unit (Fig. 2.22). These observations suggest that Fe oxide metasomatism may be genetically related to Na-Ca alteration. If this is the case, then the metasomatic Fe oxide metasomatism in outcrop may be older than magnetite precipitation associated with Cu-Au mineralisation at Ernest Henry as the latter post-dates Na-Ca alteration. The origin of the Fe oxide-rich rock outcrop situated to the east is even less clear. The outcrop is roughly 1 m wide by 4 m long and is composed almost entirely of magnetite. No textures are observed to indicate whether it formed by primary or secondary processes, although the lack of bedding or igneous textures indicates a likely metasomatic origin. The relationship between Fe oxide metasomatism and Na-Ca alteration in outcrop is investigated further in chapter 5.

At FC4NW, Fe oxide metasomatism exhibits a close spatial and temporal relationship to clinopyroxene-rich Na-Ca alteration (Fig. 2.6j and k). This is supported by their similar mineralogy, although hedenbergite (Mg No. = ~42), rather than diopside, is dominant within the Fe oxide-rich assemblages. Other minerals associated with Fe oxide metasomatism at FC4NW include albite, titanite and minor pyrite. One Fe oxide-rich interval in particular (MFC99090D 252 – 268 m) contains disseminated chalcopyrite in addition to minor actinolite (Fig. 2.19d). The presence of actinolite in

this Fe oxide-rich interval suggests that the chalcopyrite is associated with amphibole-rich Na-Ca alteration (described above) and represents a later overprint of the Fe oxide-rich rock.

While magnetite precipitation is spatially associated with clinopyroxene-rich Na-Ca alteration at FC4NW, Figures 2.5b and h show that Fe oxide-rich rocks and Na-Ca alteration at FC12 exhibit no spatial association. Furthermore, Fe oxide-rich rocks at FC12 contain only trace amounts of chalcopyrite, and contain textures that are more reminiscent of igneous processes rather than Fe oxide metasomatism. This is discussed further in chapter 5.

2.6.4. Hematite-stained K-feldspar /albite ‘red-rock’ alteration

Typically referred to as ‘red rock’ alteration due to its brick red colour in hand specimen, this represents the last major phase of alteration observed in the MFC exploration lease. Red-rock alteration represents both hematite-stained albite and K-feldspar alteration, where both can be identified by GADDS or electron microprobe analysis. At FC4NW, FC12 and outcrop, hematite-stained albite is the dominant red-rock alteration style although minor occurrences of K-feldspar alteration also occur. Hematite-stained albite and K-feldspar alteration occur with quartz and carbonate both as thin veins (1-3 cm wide) and as a pervasive replacement (Fig. 2.10e, 2.11f, 2.19f) (Williams and Blake, 1993). K-feldspar alteration is well preserved in part of the detailed mapped area of outcrop (Fig. 2.21), and is predominantly structurally controlled (as described above). The distribution of hematite-stained K-feldspar and albite alteration at FC4NW and FC12 is presented in figures 2.5d and 2.6d. Their distribution at both prospects is very broad, but appears to be more intense where Na-Ca alteration is present.

2.7. GEOCHEMICAL CHARACTERISTICS OF THE MOUNT FORT CONSTANTINE AREA

This section discusses the whole rock geochemistry from down-hole assay data at both the FC4NW and FC12 prospects. The aim is to assess the relations between the nature, distribution and timing of hydrothermal alteration, and various host rocks, intrusions and structures. Half-core samples used for whole rock geochemistry were made up of intervals between 1 to 2 m. These interval sizes were chosen by MIMEX irrespective of

the geology (for routine exploration) and therefore in most cases represent a composite of rock types and alteration suites. Elements measured from the FC4NW prospect include As, Ba, Co, Cu, Fe, Mo, Ni, P, Pb, S, Zn and K, whereas at the FC12 prospect Cu, Co, Fe and K were measured in every hole at 1 – 2 m intervals, while As, Ba, Mo, Ni, P, Pb and Zn concentrations were only determined within specific intervals containing high levels of Fe oxide. The spatial relationships between rock geochemistry and the distribution of alteration are shown in figures 2.23-2.24.

2.7.1. FC4NW

The first and most important aspect of this geochemical study involves the apparent poor correlation between Fe (>10 wt%) -Cu and Fe (>10 wt%) -S (Figs. 2.25d and i). This supports the interpretation that the timing of chalcopyrite precipitation differs from the extensive Fe oxide metasomatism. Most of the high Cu concentrations are associated with intervals containing 5 – 10 wt % Fe, reflecting the presence of chalcopyrite, pyrite, actinolite and minor magnetite within amphibole-rich Na-Ca veining and/or the host rock. Figure 2.23b illustrates further the correlation between amphibole-rich Na-Ca alteration and Cu. Cu grade is slightly higher toward the SW where amphibole-rich Na-Ca alteration is also more prominent. Cu correlates well with S, Co and Ni (Fig. 2.25b, c, e), with the S-Cu correlation largely manifest by chalcopyrite (Fig. 2.25e). A bi-plot of Ni vs Co (Fig. 2.25a) shows three main populations that exhibit varying Ni:Co ratios. As pyrrhotite is rare, the variation in these ratios may represent Co and Ni partitioning into pyrite, chalcopyrite and magnetite, respectively. Figures 2.23g and h show a consistent increase in Co and Ni downhole that correlates with pyrite.

Arsenic concentrations are typically between 5 and 20 ppm, with one interval containing 57 ppm (Fig. 2.25f). These low As values coincide with low to below detection limit Au. This differs from typical IOCG deposits where Au grades tend to be higher, for example, at the Starra Au-Cu deposit (up to 3.8 g/t) (Rotherham, 1997; Williams et al., 2001). Trace element mineral chemistry (chapter 6) indicates the presence of As in pyrite, suggesting the weakly positive correlation between Fe and As (Fig. 2.25f) is probably controlled by the distribution of pyrite, which is mostly associated with amphibole-rich Na-Ca alteration. The high As peaks exhibited in figure 2.23f may represent trace arsenopyrite not observed in thin section.

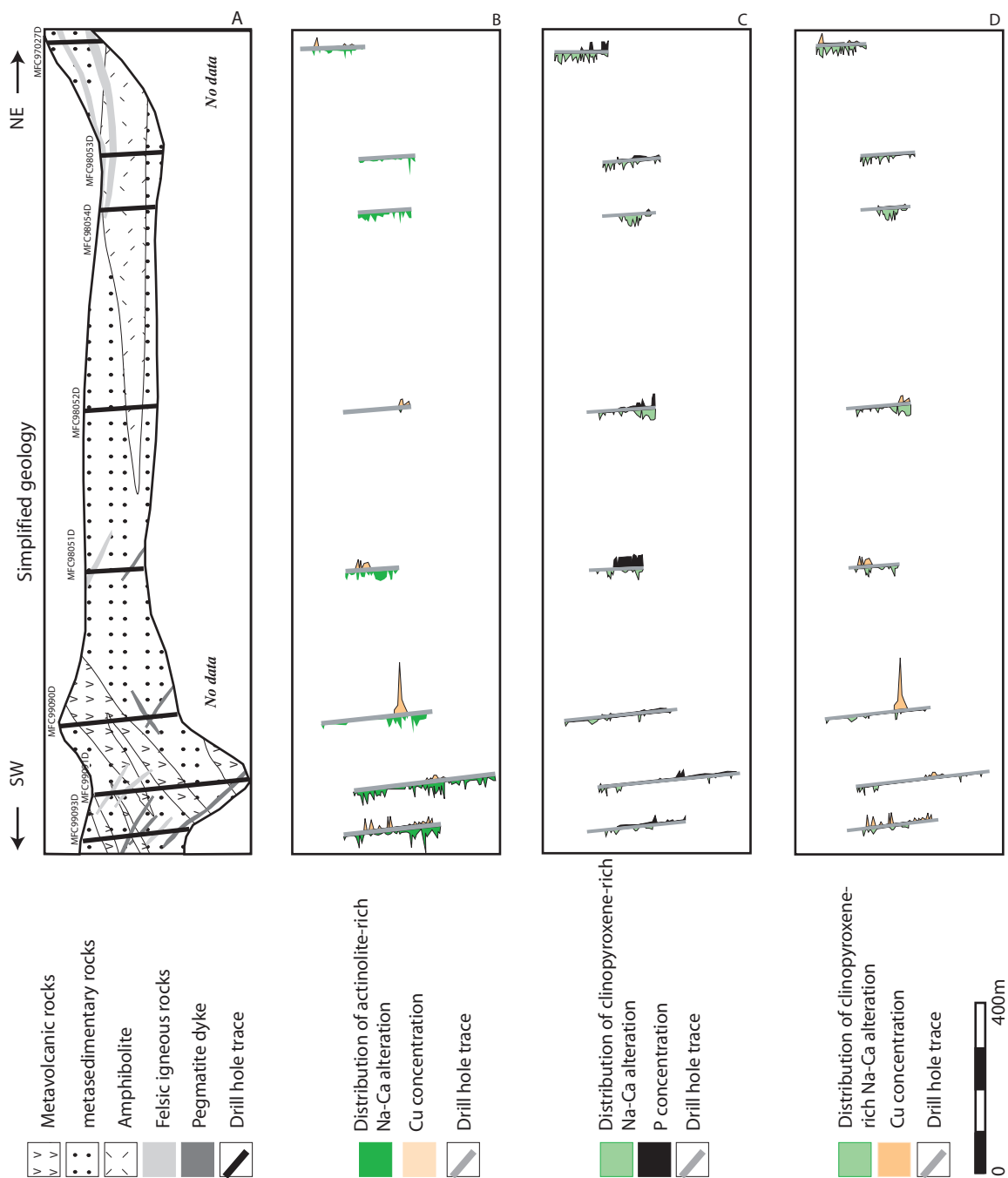


Figure 2.23. Down-hole projection of the FC4NW prospect drill holes showing correlations between hydrothermal alteration phases and chemical compositions.

A. Rock types.

B. Distribution of amphibole-rich Na-Ca alteration and Cu concentration showing a strong positive correlation. Most of the chalcopyrite at FC4NW is associated with amphibole-rich Na-Ca alteration.

C. Distribution of clinopyroxene-rich Na-Ca alteration and P concentrations showing a moderate correlation. Apatite is commonly associated with clinopyroxene-rich Na-Ca alteration.

D. Distribution of clinopyroxene-rich Na-Ca alteration and Cu concentration. The correlation here is negative as most of the chalcopyrite is associated with the later amphibole-rich Na-Ca alteration.

-Mineral assemblages and assay data are displayed as line graphs along each drill trace. These plots were generated using GOCAD where the distance of each line graph plots with respect to the drill trace indicates the relative abundance and/or concentration of the representative element or mineral.

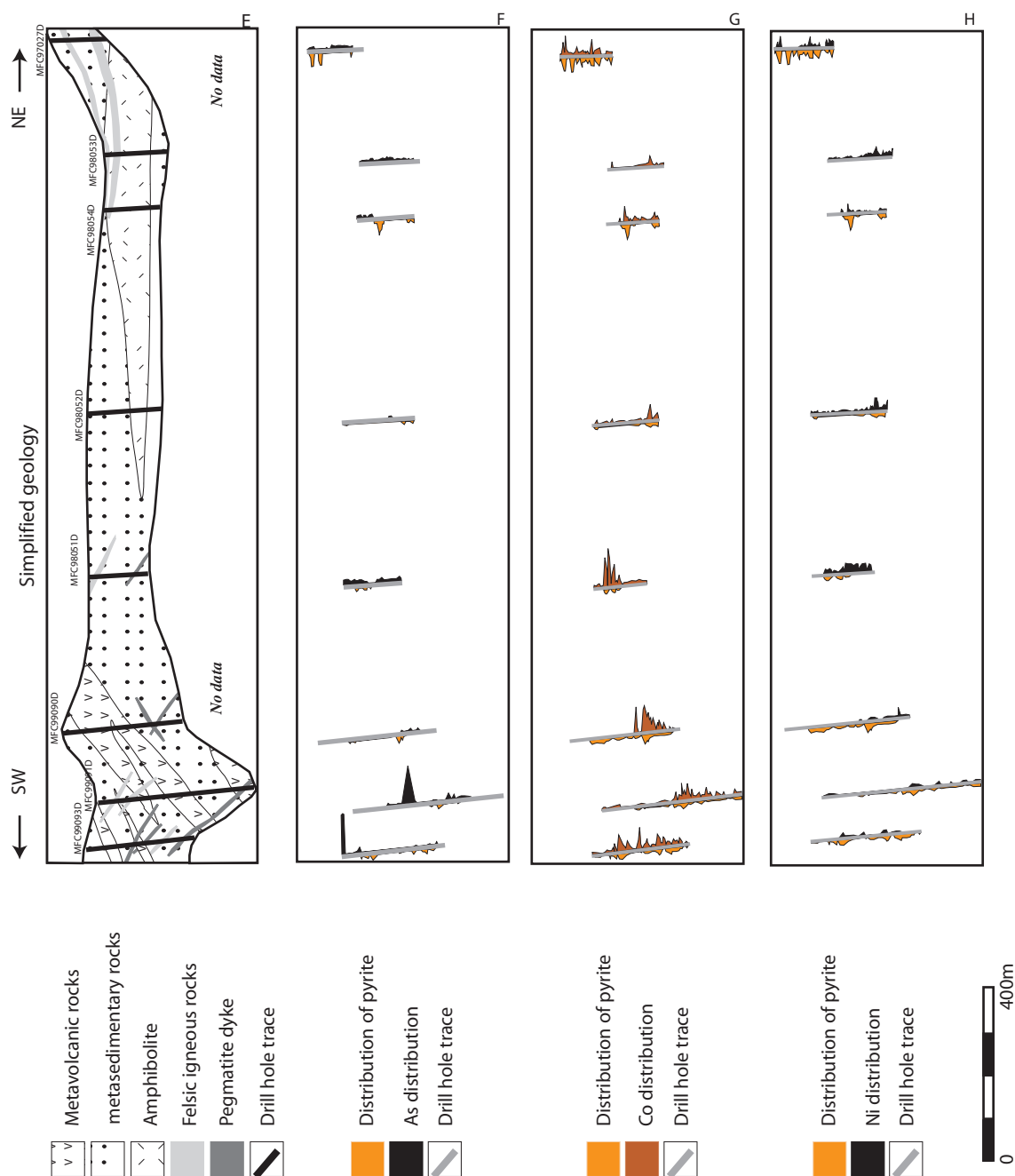


Figure 2.23 (cont). Down-hole projection of the FC4NW prospect drill holes showing correlations between hydrothermal alteration phases and chemical compositions.

E. Rock types.

F. Distribution of pyrite and As concentrations showing a moderate to strong positive correlation. This is attributed to As preferentially partitioning into pyrite.

G. Distribution of pyrite and Co concentrations showing a strong positive correlation. This is attributed to Co partitioning into pyrite.

H. Distribution of pyrite and Ni showing a moderate correlation. This is attributed to Ni partitioning into pyrite.

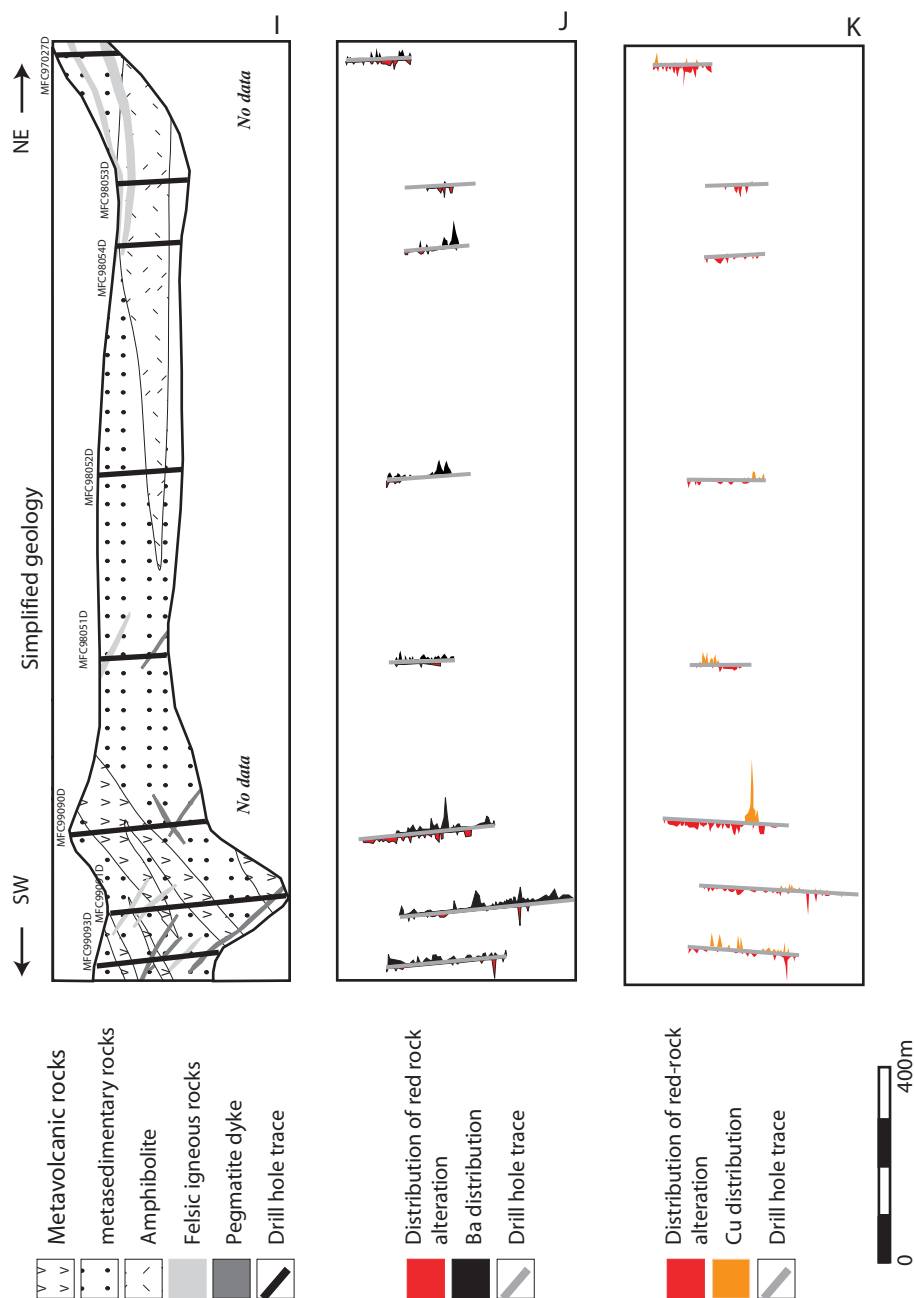


Figure 2.23 (cont). Down-hole projection of the FC4NW prospect drill holes showing correlations between hydrothermal alteration phases and chemical compositions.

I. Rock types.

J. Distribution of red rock alteration and Ba concentrations showing a positive correlation. This is attributed to the Ba content of hematite-stained K-feldspar as indicated by electron microprobe (table 2.1)

K. Distribution of red rock alteration and Cu concentrations showing a poor correlation. This poor correlation is attributed to chalcopyrite associated with the earlier amphibole-rich Na-Ca alteration.

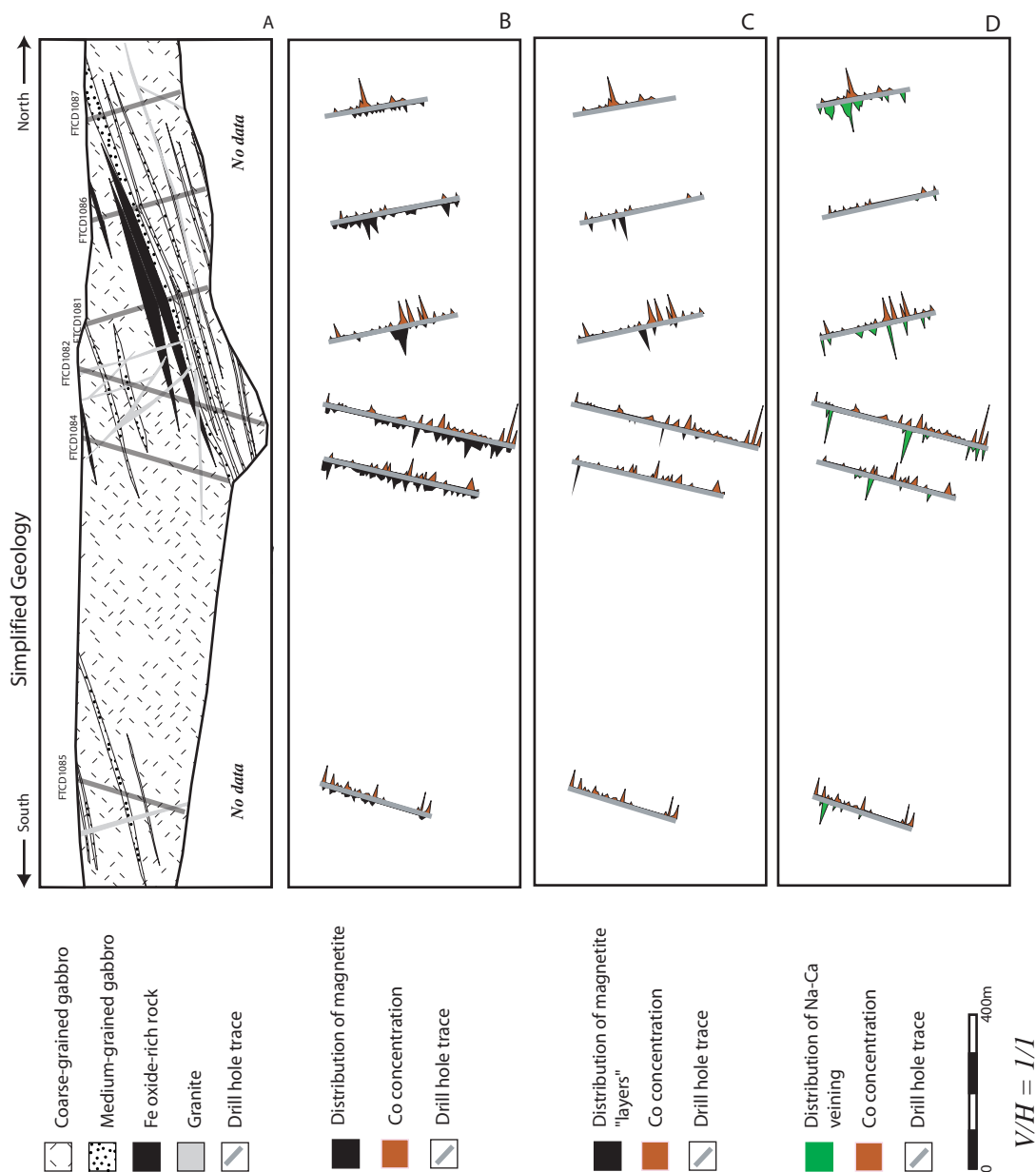


Figure 2.24. Down-hole projection of the FC12 prospect drill holes showing correlations between hydrothermal alteration phases and chemical compositions.

A. Rock types.

B. Distribution of magnetite and Co concentrations showing a positive correlation. This correlation reflects the partitioning of Co into magnetite.

C. Distribution of 'cumulate' magnetite ironstones and Co concentrations showing a positive correlation. This correlation reflects the partitioning of Co into magnetite.

D. Distribution of Na-Ca veining and Co shows a moderate to strong positive correlation. This reflects the partitioning of Co into Fe oxide and Fe sulphide minerals associated with amphibole-rich Na-Ca alteration.

- Mineral assemblages and assay data are displayed as line graphs along each drill trace. These plots were generated using GOCAD where the distance of each line graph plots with respect to the drill trace indicates the relative abundance and/or concentration of the representative element or mineral.

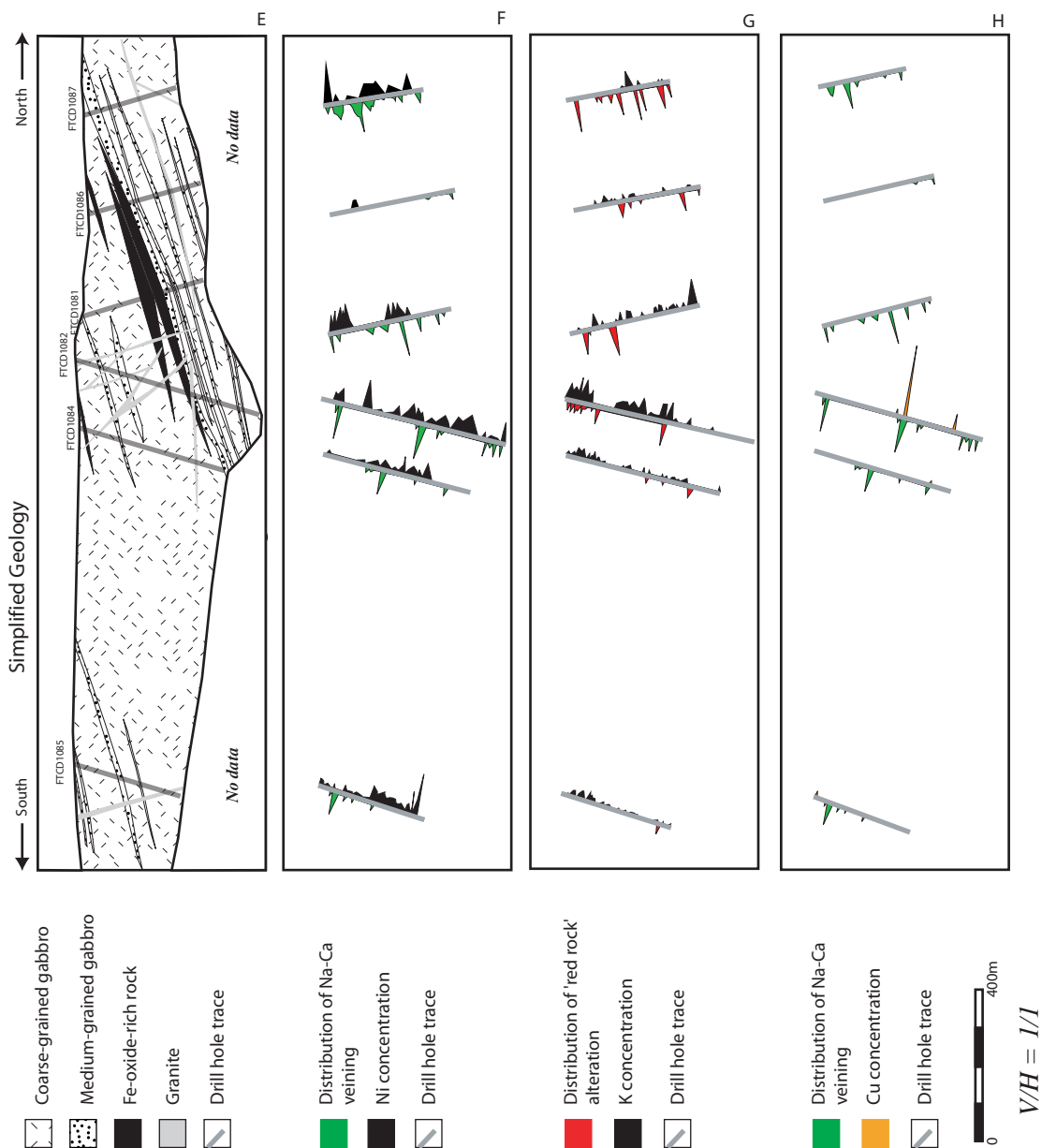


Figure 2.24 (cont). Down-hole projection of the FC12 prospect drill holes showing correlations between hydrothermal alteration phases and chemical compositions.

E. Rock types.

F. Distribution of Na-Ca veining and Ni concentration showing a moderate to strong positive correlation. This reflects the partitioning of Ni into Fe oxide and Fe sulphide minerals associated with amphibole-rich Na-Ca alteration.

G. Distribution of 'red rock' alteration and K showing a poor correlation. This is likely to be due to red rock alteration at FC12 predominately composed of hematite-stained albite alteration rather than hematite-stained K-feldspar alteration.

H. Distribution of Na-Ca veining and Cu concentrations showing a positive correlation. Most of the chalcopyrite at FC12 is associated with amphibole-rich Na-Ca alteration.

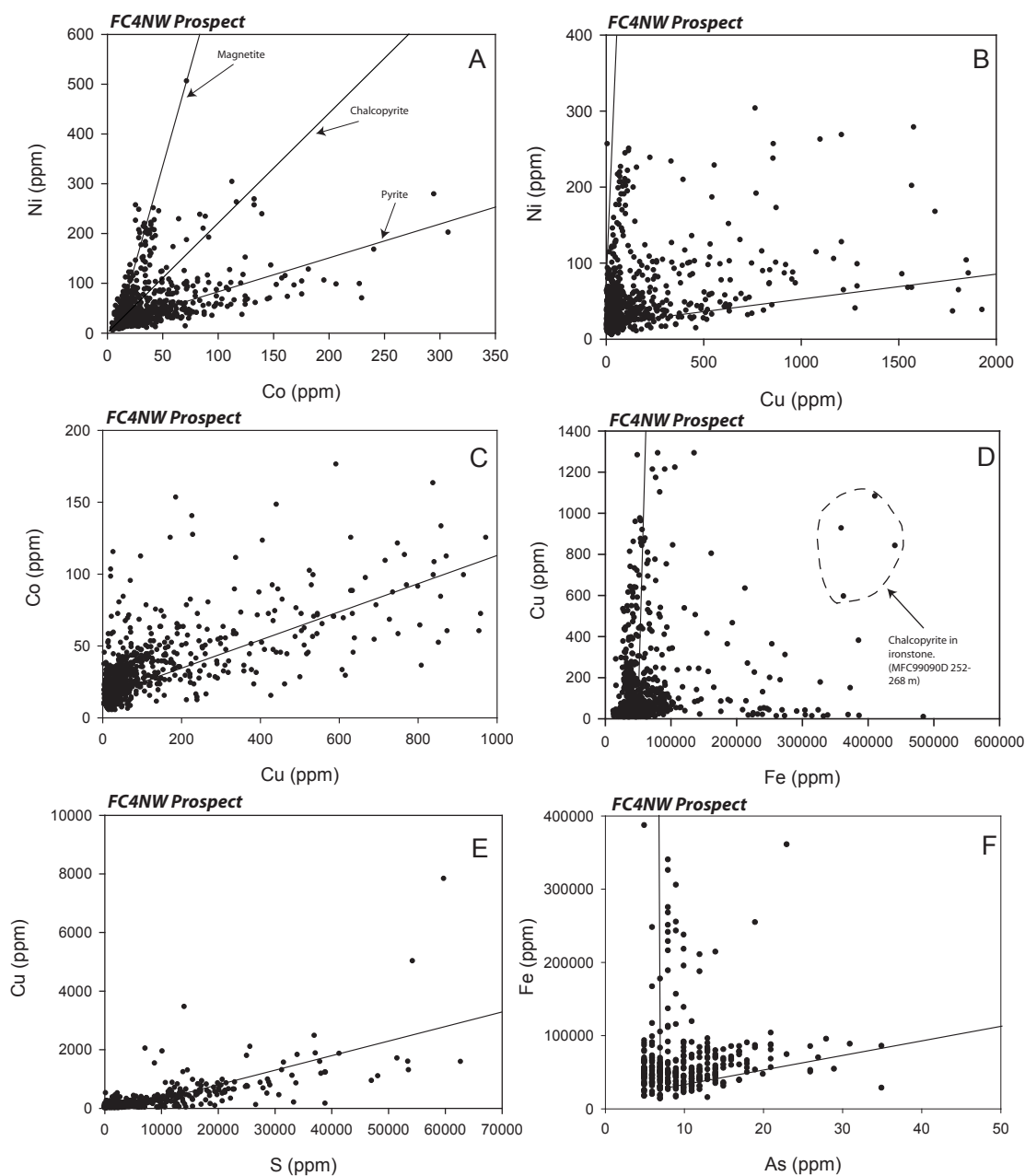


Figure 2.25. Whole rock geochemistry of rocks from the FC4NW prospect:

A: Co vs Ni: three subpopulations due to Co and Ni partitioning into magnetite, chalcopyrite and pyrite.

B: Cu vs Ni: shows two positive correlation trends due to Ni partitioning into chalcopyrite and pyrite.

C: Cu vs Co: a positive correlation due to Co partitioning into chalcopyrite.

D. Fe vs Cu: A correlation between Cu and Fe (<10 wt %) due to the association between chalcopyrite and Fe-bearing minerals (magnetite, pyrite) within amphibole-rich Na-Ca alteration.

E. S vs Cu: positive correlation highlighting the presence of chalcopyrite.

F. Fe vs As: positive correlation attributed to arsenic partitioning into pyrite.

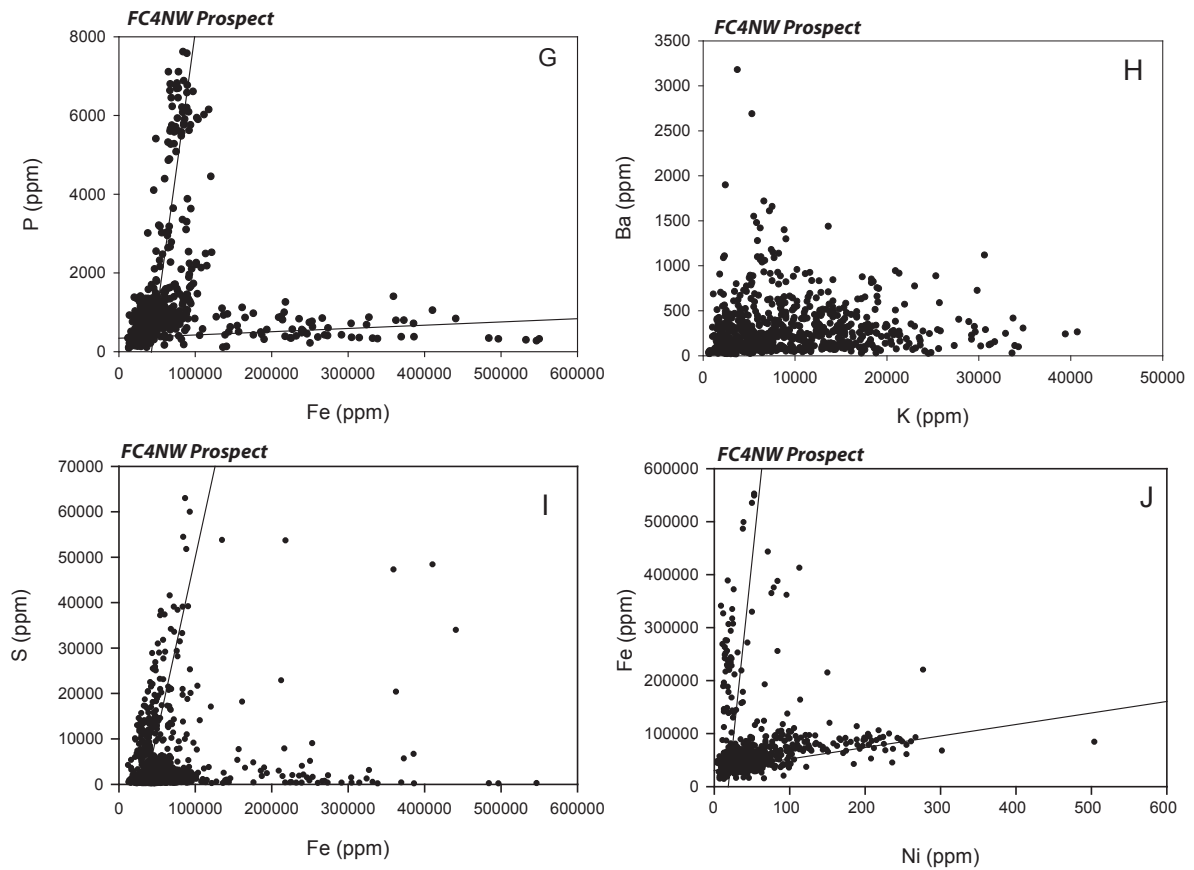


Figure 2.25 (cont). Whole rock geochemistry of rocks from the FC4NW prospect
G. Fe vs P: poor correlation attributed to the absence of apatite during Fe oxide metasomatism.

H. K vs Ba: weak positive correlation between K and Ba attributed to Ba in K-feldspar (c.f. electron microprobe in table 2.1)

I. Fe vs S: correlation between S and Fe (<10 wt %) due to pyrite and chalcopyrite.

J. Ni and Fe: two populations with different Ni:Fe ratios indicating Ni partitioning into magnetite and pyrite.

The distribution of hematite-stained K-feldspar and albite alteration appears to coincide with the presence of earlier albitisation. Figure 2.23j shows a weak correlation between Ba enrichment and the distribution of red-rock alteration. This supports the interpretation that some of the 'red-rock' alteration at FC4NW is composed of K-feldspar as Ba will partition strongly into this particular mineral.

2.7.2. FC12

The geochemical variation at FC12 is similar to the FC4NW prospect described above. A negative correlation between Cu and Fe is shown in figure 2.26a, whereby the highest Cu concentrations lie in intervals containing 5-15 wt % Fe. In contrast, intervals containing up to 60 wt % Fe contain considerably less Cu. This provides further evidence that the formation of Fe oxide-rich rocks is unrelated to the Cu mineralisation at FC12 and instead is associated with Na-Ca alteration (Fig. 2.24h). Positive correlations also exist between Fe, Ni and Co. This correlation is divided into two populations (Fig. 2.26b, c), and is likely to reflect the partitioning of these elements into magnetite and pyrite (chapter 6). This is supported by figure 2.24b where high Co is also associated with abundant magnetite, and figures 2.24d, f where Ni and Co show a strong positive correlation with sulphide-bearing Na-Ca veins. A weak positive correlation exists between K and Ba (Fig. 2.26d), reflecting that dominance of hematite-stained albite over K-feldspar alteration at FC12.

2.8. COMPARISONS WITH THE ERNEST HENRY CU-AU SYSTEM AND OTHER FE-OXIDE CU-AU DEPOSITS

This section compares the geology, paragenetic history and geochemistry of the MFC exploration lease with previous work from the Ernest Henry deposit (Mark et al, 1999) and regional Na-Ca alteration elsewhere in the EFB (e.g. Fullarton River Gouge; de Jong and Williams, 1995; Oliver et al., 2004). A comparison between the MFC exploration lease and Fe oxide (\pm Cu-Au) occurrences elsewhere in the EFB are summarised in table 2.2, and the regional context of Na-Ca alteration is shown in figures 2.2 and 2.3.

2.8.1. Rock types

Metavolcanic rocks in outcrop at MFC commonly contain both quartz and plagioclase phenocrysts. In contrast, metavolcanic rocks at Ernest Henry are dominated by

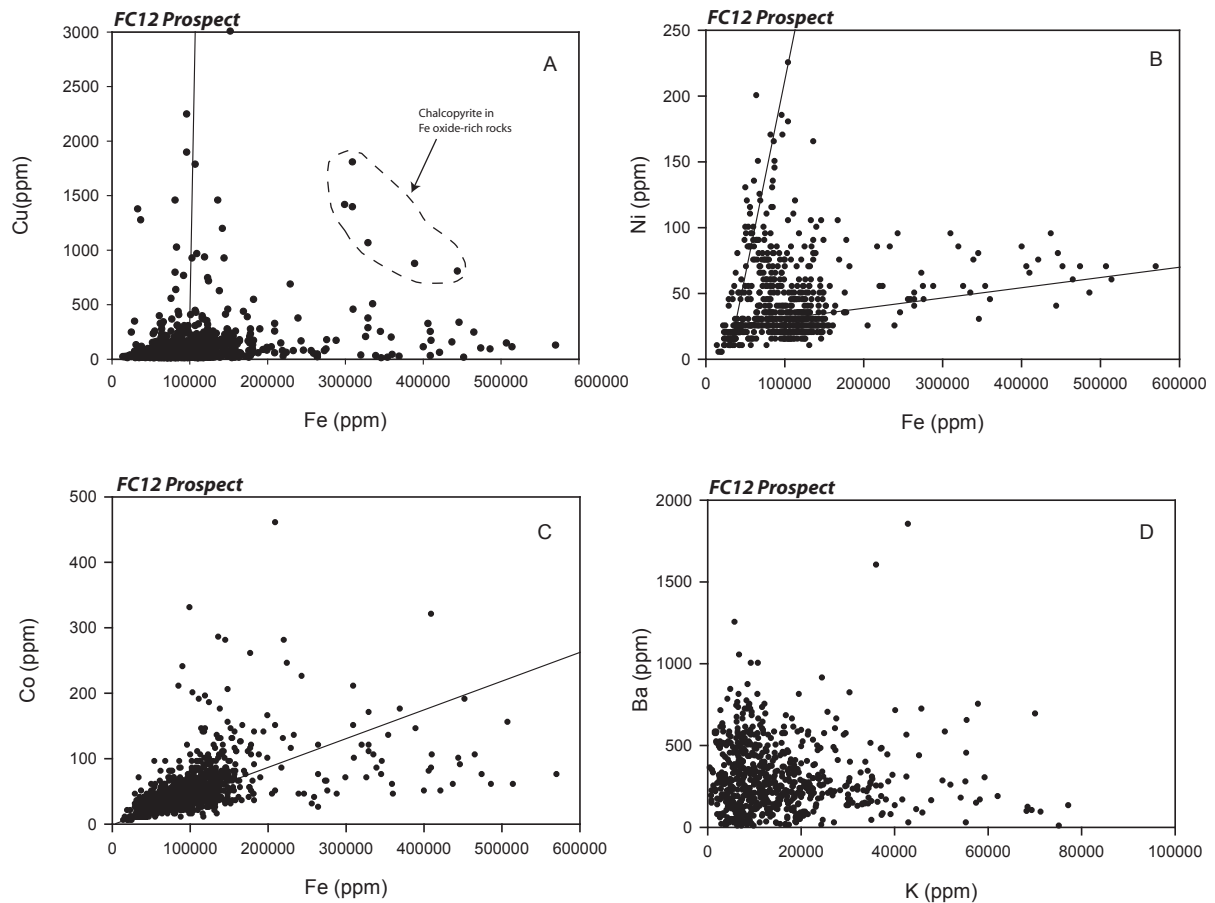


Figure 2.26. Whole rock geochemistry of samples from the FC12 prospect
A. Fe vs Cu: weak positive correlation between Cu and Fe (< 10 wt %) attributed to chalcopyrite within amphibole-rich Na-Ca alteration .
B. Fe vs Ni: two populations exhibiting positive correlations indicating Ni partitioning into magnetite and pyrite.
C. Fe vs Co: positive correlation between Co and Fe attributed to Co partitioning into pyrite and magnetite.
D. K vs Ba: weak positive correlation between K and Ba attributed to Ba in K-feldspar.

Mount Fort Constantine Vs Ernest Henry

	<i>Ernest Henry Cu-Au deposit</i>	<i>FC4NW prospect</i>	<i>FC12 prospect</i>	<i>MFC outcrop</i>	<i>Other IOCG deposits (i.e. Starra, Osborne)</i>
Aeromagnetic response (see figure 2.4)	Highly magnetic	Moderately magnetic	Highly magnetic	Moderately magnetic	Variable depending on whether Fe oxide is hematite or magnetite
Host rocks to Cu±Au mineralisation	Plagioclase phyric felsic volcanic rocks Minor calc-silicates, diorites	Metasedimentary / calc-silicate rocks Amphibolites Felsic volcanic rocks Granitic rocks	Tholeiitic gabbroic rocks	No Cu-Au mineralisation	Pelites, psammites, amphibolites
Fe oxide-rich rocks (ironstones)	<i>Multiple events:</i> Fe-K alteration: pre mineralisation (magnetite) Cu-Au mineralisation (magnetite)	<i>One event:</i> Clinopyroxene / magnetite-rich Na-Ca alteration (magnetite) Pre-dates Cu-Au mineralisation at Ernest Henry	<i>One event:</i> Igneous or metasomatic origin(?) (see chapter 5) Pre-dates Cu-Au mineralisation at Ernest Henry	<i>One event (?):</i> Timing unclear; probably related to Na-Ca alteration Pre-dates Cu-Au mineralisation at Ernest Henry (?)	<i>Multiple events:</i> Early barren ironstones (Western and banded ironstones) Cu-Au mineralisation (magnetite)
Major Cu±Au mineralisation event	Post Na-Ca alteration Infill in breccia matrix Complex geochemistry and mineralogy	Actinolite-rich Na-Ca alteration Infill within brittle veins / localised breccia zones Disseminated in alteration haloes	Na-Ca alteration and veining Infill within brittle veins	No Cu-Au mineralisation observed	Post Na-Ca alteration Temporally associated with Williams-Naraku Batholith
Geochemical characteristics	Strong Cu-Au / Fe-Cu / K-Ba correlation (+ve) Strong Fe, S, Mo, Co, As, U correlation with Cu-Au (+ve) Weak Ni, Mn correlation with Cu-Au mineralisation (+ve)	No Cu-Au correlation Poor Fe-Cu correlation (+ve) Weak K-Ba correlation (+ve) Strong Co/Fe correlation (+ve) Strong Ni/Cu correlation (+ve) Weak Fe/P correlation (+ve)	No Cu-Au correlation No Fe-Cu correlation Strong Ni-Fe correlation (+ve) Strong Co-Fe correlation (+ve) Weak K-Ba correlation (+ve)	No data available	Osborne: Cu-Au correlates with Ag, Co, Ni, Mo, Se, Hg, Bi and Te
Post-peak metamorphic intrusive rocks	None	Na-rich granitic intrusions Pegmatitic dykes	Na-rich granitic intrusions	No observed igneous intrusions	Intrusions at Mt Elliott Distal elsewhere

Table 2.2. Attributes of various IOCG deposits, including Ernest Henry, and the areas covered in this study: FC4NW and FC12 prospects, and MFC outcrop. Ernest Henry data from Mark et al, (1999). Other sources are Rotherham (1997) for Starra and Adshead (1995) for Osborne. Abbreviation ‘ve’ represents positive or negative correlation.

plagioclase phenocrysts only (Mark et al., 1999), suggesting the rocks at MFC may represent a more evolved volcanic unit. Metavolcanic rocks at FC4NW are strongly affected by numerous hydrothermal events making it difficult to ascertain the primary characteristics of unaltered equivalents. Rare, slightly altered rocks resemble the fine- to medium-grained plagioclase-phyric volcanic rocks characterised as 'group 2' by Mark et al., (1999). Metavolcanic rocks at both Ernest Henry and FC4NW are intercalated with scapolitic-calc-silicate rocks suggesting these rocks are part of the same stratigraphic interval and thus likely to have similar ages, *ca.*1745 Ma (crystallisation ages for volcanic rocks at MFC are 1746 ± 8 Ma and 1742 ± 6 Ma; Page and Sun, 1998).

The three areas focussed on within the MFC exploration lease (FC12/FC4NW prospects and outcrop) all contain a variety of rock types that may have influenced the availability and transport of fluids responsible for Cu-Au mineralisation. The FC4NW prospect in particular is dominated by metasedimentary and calc-silicate rocks, with moderate occurrences of felsic volcanic rocks to the southwest and amphibolite to the northeast. Amphibole-rich Na-Ca alteration hosting chalcopyrite at FC4NW predominately occurs as brittle veins. In contrast, felsic volcanic rocks host Cu-Au mineralisation at Ernest Henry, and are highly brecciated due to their relatively high competency, enhanced by albitisation. This brecciation provided space for the precipitation of Cu-bearing minerals from the mineralising fluid (Mark et al., 1999). It could be argued that the metasedimentary rocks at FC4NW reduced the likelihood of brecciation occurring due to their relatively low competency compared to felsic volcanic rocks from Ernest Henry, resulting in a lack of open space needed to focus Cu-Au-enriched fluids. However, numerous workers (Oliver, 1995; Marshall, 2003) have documented the brecciation of less competent rocks within the Cloncurry district and the Mary Kathleen Fold Belt. Marshall (2003) argued that a major factor controlling brecciation within the Cloncurry district is the relative competency contrast between adjacent layers in calc-silicate rocks during D₂ and D₃ deformation. In general, rocks within the Cloncurry district (*ca.* 450-550°C) are significantly more brecciated compared to similar rocks within the Mary Kathleen Fold Belt (*ca.* 550-650°C). The occurrence of widespread brecciation in rocks of contrasting competency indicates that

mechanical attributes are not likely to be a major factor responsible for the lack of significant Cu-Au mineralisation in any of the areas of study.

2.8.2. Igneous intrusions

Another significant difference between the Ernest Henry Cu-Au deposit and the FC4NW and FC12 prospects is the absence of proximal post-peak metamorphic intrusive rocks at the time of Cu-Au mineralization at Ernest Henry. In contrast, several granitic intrusive rocks were observed at FC4NW, along with one early intrusive phase at the FC12 prospect (similar to Na-rich granitic rocks observed at Mt Margaret). The presence of post-peak metamorphic intrusive rocks at FC12 and FC4NW implies the presence of an adjacent major igneous body (Williams-Naraku batholith?) as suggested by figure 2.4. The absence of significant post-peak metamorphic intrusive rocks at Ernest Henry and other IOCG deposits (with the exception of Mt Elliott) suggests a more distal spatial relationship to coeval intrusions (intrusions near Ernest Henry shown in figure 2.4 are pre-metamorphic).

The Lightning Creek Cu-Au prospect contains subeconomic Cu mineralisation that is hosted within granitic rocks and Fe-rich sills. PIXE (Photon Induced X-ray Emission) and conventional microthermometric analysis of fluid inclusions by Perring et al. (2000) revealed minimum trapping temperatures of 420 to 495°C and high levels of Cu (~1 wt %) in the fluid. Importantly, these Cu levels are higher than in fluid inclusions from most other IOCG deposits in the EFB. Perring et al (2000) suggested that the lack of significant Cu-Au mineralisation is likely to be a product of high temperatures and/or a lack of sulphur in the fluids or host rock. If specific thermal conditions were required for Cu-Au mineralisation to occur, then perhaps the FC4NW and FC12 prospects are situated too close to the source of magmatic fluids responsible for Cu-Au mineralisation (i.e. igneous intrusion). Additionally, a lack of sufficient S may have prevented the precipitation of Cu-bearing sulphides. Ernest Henry may have had more appropriate thermal conditions and/or sufficient S for the deposition of Cu-Au mineralisation. This issue is investigated further in chapter 4.

2.8.3. Alteration and geochemistry

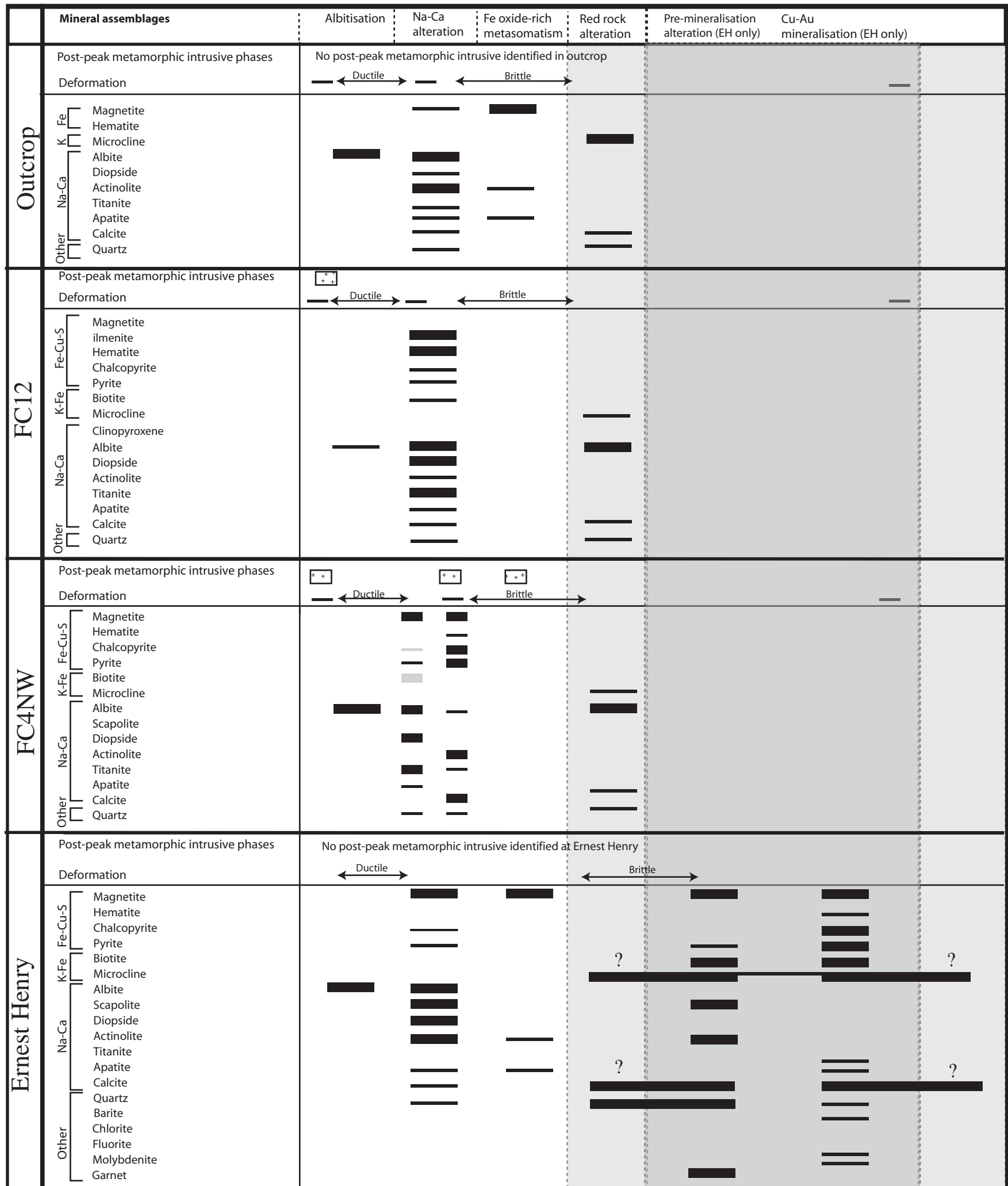


Figure 2.27 Paragenesis of major alteration phases at the FC12 and FC4NW prospects and MFC outcrop compared to the Ernest Henry hydrothermal system. Relationships to post-peak metamorphic intrusive rocks and styles of deformation are also shown. Note minerals represented by grey bars in the FC4NW prospect occur in association with coarse-grained biotite alteration only. Grey area represents pre- and syn- Cu-Au mineralisation phases at Ernest Henry which are not observed in outcrop or at the FC12 and FC4NW prospects

The alteration packages observed at both Ernest Henry and MFC can be combined into the following sequential categories according to similar mineralogies and textures (Fig. 2.27):

1. Albitisation
2. Na±Ca alteration (Main phase of sulphide mineralisation at FC4NW and FC12)
3. Fe oxide-rich metasomatism (MFC outcrop) and hanging wall Fe oxide-rich rocks at Ernest Henry.
4. 'Red-rock' alteration (hematite-stained and / or K-feldspar alteration). This alteration may represent overlapping phases that occur both during and after the main phase of Cu-Au mineralisation (6).
5. Pre-mineralisation: Garnet-K-feldspar-biotite-magnetite-pyrite veining and alteration (Ernest Henry only)
6. Cu-Au mineralisation (Ernest Henry only)

The Ernest Henry deposit contains a more mineralogically and chemically complex hydrothermal alteration history than those observed in outcrop at MFC and within the FC4NW and FC12 prospects. This is clearly evident from comparisons of the paragenesis for each area (Fig. 2.27). The most notable difference is the relatively complex mineralogy associated with the Cu-Au mineralisation phase at Ernest Henry compared to the FC12 and FC4NW prospects. There is also a strong positive correlation between Cu and Au at Ernest Henry providing evidence that Au is closely associated with chalcopyrite. This correlation is not apparent within the FC4NW or FC2 prospects, where Au is mostly below detection. Ernest Henry also exhibits a strong positive correlation between Fe and Cu, reflecting the co-precipitation of magnetite and chalcopyrite during the main phase of Cu-Au mineralisation (Mark et al., 1999). The formation of Fe oxide-rich rocks at FC4NW and FC12 is not related to chalcopyrite precipitation as illustrated by the poor Cu-Fe correlation at both prospects. Instead, Fe oxide-rich rocks are related to an earlier phase of clinopyroxene-rich Na-Ca alteration at FC4NW, whereas at FC12, Fe oxide-rich rocks may have formed by other processes besides Fe oxide metasomatism (discussed in chapter 5). Additionally, the barren Fe oxide-rich outcrop may be related to Na-Ca alteration indicated by their similar mineralogy. Chalcopyrite at FC12 and FC4NW is precipitated within amphibole-rich Na-Ca veins that contain minor magnetite on the vein margins only.

Several aspects of the paragenesis at Ernest Henry, FC12, FC4NW and outcrop are similar and include the following:

1. Early albitisation
2. Na-Ca alteration
3. Relatively Cu-poor Fe oxide formation
4. Hematised K-feldspar / albitic alteration.

Each of these alteration phases is abundant throughout the EFB. Na-Ca alteration and veining peripheral to the Ernest Henry deposit contains a similar mineral composition to regional Na±Ca alteration described by de Jong and Williams (1995), Tolman (1998) and Mark, (1998a,b) and within the MFC exploration lease. It is possible, therefore, that Na-Ca alteration peripheral to the Ernest Henry deposit and at MFC may both be related to the same Na-Ca alteration event (discussed further in chapters 3 and 4). A positive correlation between K and Ba is observed at Ernest Henry whereas only a weak positive correlation is observed at FC4NW and FC12. Additionally, Mark et al (1999) documented Ba concentrations of 1 to 1.5 wt% in K-feldspar at Ernest Henry, higher than Ba concentrations at FC4NW and in outcrop (0.8 wt % Ba). The relationship between 'red rock' alteration within the MFC exploration lease with respect to Ernest Henry is problematic. Mark et al (in press) showed that hematised K-feldspar veins from the Cloncurry Fault may have formed from low-latitude meteoric fluids as young as *ca.* 1100 Ma or later. Alternatively, hematised K-feldspar alteration at Ernest Henry mostly pre-dates Cu-Au mineralisation (>1510-1500 Ma; Twyerould, 1997). This implies that hematite-stained albite and K-feldspar alteration at FC4NW and FC12 may range anywhere between >1510 to 1100 Ma. Despite the large range of ages, if 'red-rock' alteration at Ernest Henry and MFC are all temporally related, an estimation of the relative timing of Cu-Au mineralisation at Ernest Henry compared to the paragenesis at MFC can be made. From this assumption, Cu-Au mineralisation most likely formed after the hematised K-feldspar/albite alteration event at FC4NW, FC12 and outcrop (Fig. 2.27).

2.9. DISCUSSION AND CONCLUSIONS

Hydrothermal alteration within the FC4NW and FC12 prospects and in outcrop is hosted in a variety of rock types. The FC12 prospect is composed of coarse-grained gabbroic rocks intercalated with fine- to medium- grained gabbroic rocks. At FC4NW, the dominant rock types include calc-silicate and metasedimentary rocks, although plagioclase-phyric felsic volcanic rocks (similar to those observed at the Ernest Henry deposit) and amphibolite occur towards the south-west and north-east respectively. Quartz-plagioclase-phyric felsic volcanic rocks and minor calc-silicate rocks are also exposed in outcrop. Post-peak metamorphic felsic igneous rocks intrude all rock types within the FC12 and FC4NW prospects, and exhibit an intimate temporal relationship with Na-Ca alteration, particularly at FC4NW. Felsic igneous rocks were not observed in outcrop.

Several different alteration phases were identified within the MFC exploration lease. Na-Ca alteration, similar to that observed at Ernest Henry and on a regional scale, is the most pervasive style. Na-Ca alteration at FC12 and FC4NW is also the main host to sulphide mineralisation. Na-Ca alteration at FC4NW occurs as two distinct phases:

1. *Clinopyroxene-rich alteration*, which occurs as a ductile-brittle style vein and alteration phase that is more pervasive toward the north-east; and,
2. *Amphibole-rich alteration*, which overprints type 1 and is more prevalent towards the south-west of the area.

Amphibole-rich Na-Ca alteration is observed at FC12 and occurs as brittle veins that exhibit distinct zoning in mineral abundance from magnetite, actinolite, albite, titanite at the vein margins to calcite, albite, specular hematite, pyrite and chalcopyrite rich cores. In outcrop, amphibole-rich Na-Ca alteration commonly occurs as intense breccia bodies localised by shear zones and competency contrasts between albitised felsic volcanic rocks and calc-silicate rocks.

A temporal relationship between Fe oxide metasomatism and Na-Ca alteration is recognised in outcrop and at the FC4NW prospect. In outcrop, the hematite + magnetite + apatite + actinolite –rich rock exhibits a number of mineralogical similarities to Na-Ca alteration products, and as such is considered to bear some relationship to regional alteration processes. A similar relationship is also apparent at the FC4NW prospect

where the Fe oxide-rich rocks contain a mineral assemblage more closely akin to clinopyroxene-rich Na-Ca alteration, which is later overprinted by amphibole-rich veining and coincident sulphide mineralisation. Likewise, in the hanging wall of Ernest Henry, a magnetite –(apatite) Fe oxide-rich rock is co-associated with a suite of pre-ore Na-Ca altered rocks. In contrast, at the FC12 prospect, Fe oxide-rich rocks appear to have formed by other processes and are later overprinted by metamorphism and subsequent hydrothermal sulphide-bearing Na-Ca veining and alteration (chapter 5).

These observations show that Fe oxide-rich mineralisation at FC4NW and outcrop is predominantly associated with clinopyroxene- and amphibole-rich Na-Ca alteration, respectively. These two styles of hydrothermal alteration are comparable to the regionally extensive Na-Ca alteration which typically pre-dates mineralisation at most IOCG deposits, including Ernest Henry. However, in contrast to most of the IOCG deposits where sulphide mineralization is related to K enrichment, most sulphide mineralization around the Mount Fort Constantine exploration leases is associated with amphibole-rich Na-Ca alteration, similar to barren Fe oxide (apatite) bodies in the hanging wall of Ernest Henry. The geochemical data for MFC show relatively poor correlations between Fe and Cu, K and Fe, and K and Cu compared to Ernest Henry. The temporal, geochemical and mineralogical relations between both Na-Ca alteration and magmatism in the FC4NW prospect strengthen the argument for a local magmatic-hydrothermal contribution to Na-Ca fluids (Mark, 1999; Perring et al., 2000). This association also suggests that the early clinopyroxene-rich Na-Ca alteration phase (and related Fe oxide-rich rocks) formed from relatively hotter fluids than those associated with later amphibole-rich Na-Ca alteration. A thermal gradient between both Na-Ca alteration styles is also consistent with the progression from clinopyroxene to amphibole-rich assemblages, and the late timing of sulphide mineralisation.

The parageneses at FC4NW, FC12 and outcrop, and Ernest Henry show clear similarities and marked differences. Early alteration stages at Ernest Henry bare a number of similarities to early Na- and Na-Ca alteration assemblages hosting the main phase of sulphide mineralisation at FC4NW and FC12. Hematised K-feldspar and albite alteration also overprints each of these earlier alteration stages. Significantly, the complex chemistry and mineralogy associated with the main phase of Cu-Au mineralisation at Ernest Henry is absent in each of the areas studied within the MFC

exploration lease. This implies that the fluid(s) responsible for Cu-Au mineralisation were not 'seen' by the rocks at the FC4NW and FC12 prospects or in outcrop (chapter 6). Mechanical considerations alone cannot be applied to, as work by previous authors has shown that less competent rocks such as metasediments and calc-silicate rocks can still brecciate under certain conditions, particularly if they lie adjacent to a more competent rock unit and/or the rocks have been previously albitised. One possibility is that another, externally derived fluid never interacted with Na-Ca-Cu-bearing fluids at MFC, which may explain the absence of Au and other components compared to the Ernest Henry deposit. This hypothesis is investigated in the following chapters.